Chapter 1

Dynamical Systems

1.1 Introduction

1.1.1 Phase Space and Phase Curves

Dynamics is the study of motion through phase space. The phase space of a given dynamical system is described as an N-dimensional manifold, $\mathcal{M}$. A (differentiable) manifold $\mathcal{M}$ is a topological space that is locally diffeomorphic to R^N.[1] Typically in this course $\mathcal{M}$ will $\mathbf{R}^N$ itself, but other common examples include the circle S^1, the torus T^2, the sphere S^2, *etc.*

Let $g_t \colon \mathcal{M} \to \mathcal{M}$ be a one-parameter family of transformations from $\mathcal{M}$ to itself, with $g_{t=0} = 1$, the identity. We call g_t the t-advance mapping. It satisfies the composition rule

$$g_t \, g_s = g_{t+s} \ . \tag{1.1}$$

Let us choose a point $\boldsymbol{\varphi}_0 \in \mathcal{M}$. Then we write $\boldsymbol{\varphi}(t) = g_t \, \boldsymbol{\varphi}_0$, which also is in $\mathcal{M}$. The set $\bigl\{ g_t \, \boldsymbol{\varphi}_0 \bigm| t \in \mathbf{R} \, , \, \boldsymbol{\varphi}_0 \in \mathcal{M} \bigr\}$ is called a *phase curve*. A graph of the motion $\boldsymbol{\varphi}(t)$ in the product space $\mathbf{R} \times \mathcal{M}$ is called an *integral curve*.

1.1.2 Vector Fields

The *velocity* vector $\boldsymbol{V}(\boldsymbol{\varphi})$ is given by the derivative

$$\boldsymbol{V}(\boldsymbol{\varphi}) = \frac{d}{dt}\bigg|_{t=0} g_t \, \boldsymbol{\varphi} \ . \tag{1.2}$$

The velocity $\boldsymbol{V}(\boldsymbol{\varphi})$ is an element of the *tangent space* to $\mathcal{M}$ at $\boldsymbol{\varphi}$, abbreviated $\mathrm{T}\mathcal{M}_{\boldsymbol{\varphi}}$. If $\mathcal{M}$ is N-dimensional, then so is each $\mathrm{T}\mathcal{M}_{\boldsymbol{\varphi}}$ (for all $\boldsymbol{p}$). However, $\mathcal{M}$ and $\mathrm{T}\mathcal{M}_{\boldsymbol{\varphi}}$ may

[1] A *diffeomorphism* $F \colon \mathcal{M} \to \mathcal{N}$ is a differentiable map with a differentiable inverse. This is a special type of *homeomorphism*, which is a continuous map with a continuous inverse.

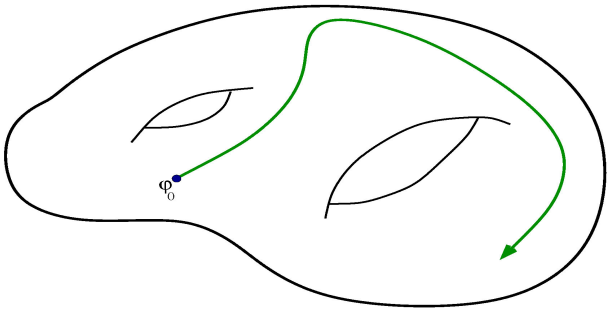

Figure 1.1: An example of a phase curve.

differ topologically. For example, if $\mathcal{M} = \mathrm{S}^1$, the circle, the tangent space at any point is isomorphic to $\mathbf{R}$.

For our purposes, we will take $\boldsymbol{\varphi} = (\varphi_1, \ldots, \varphi_N)$ to be an N-tuple, *i.e.* a point in $\mathbf{R}^N$. The equation of motion is then

$$\frac{d}{dt}\,\boldsymbol{\varphi}(t) = \boldsymbol{V}\big(\boldsymbol{\varphi}(t)\big)\ . \tag{1.3}$$

Note that any $N^{\rm th}$ order ODE, of the general form

$$\frac{d^N x}{dt^N} = F\left(x, \frac{dx}{dt}, \ldots, \frac{d^{N-1}x}{dt^{N-1}}\right)\ , \tag{1.4}$$

may be represented by the first order system $\dot{\boldsymbol{\varphi}} = \boldsymbol{V}(\boldsymbol{\varphi})$. To see this, define $\varphi_k = d^{k-1}x/dt^{k-1}$, with $k = 1, \ldots, N$. Thus, for $j < N$ we have $\dot\varphi_j = \varphi_{j+1}$, and $\dot\varphi_N = f$. In other words,

$$\overbrace{\frac{d}{dt}\begin{pmatrix}\varphi_1\\ \vdots\\ \varphi_{N-1}\\ \varphi_N\end{pmatrix}}^{\dot{\boldsymbol{\varphi}}} = \overbrace{\begin{pmatrix}\varphi_2\\ \vdots\\ \varphi_N\\ F\big(\varphi_1, \ldots, \varphi_N\big)\end{pmatrix}}^{\boldsymbol{V}(\boldsymbol{\varphi})}\ . \tag{1.5}$$

1.1.3 Existence/Uniqueness/Extension Theorems

Theorem : Given $\dot{\boldsymbol{\varphi}} = \boldsymbol{V}(\boldsymbol{\varphi})$ and $\boldsymbol{\varphi}(0)$, if each $\boldsymbol{V}(\boldsymbol{\varphi})$ is a smooth vector field over some open set $\mathcal{D} \in \mathcal{M}$, then for $\boldsymbol{\varphi}(0) \in \mathcal{D}$ the initial value problem has a solution on some finite time interval $(-\tau, +\tau)$ and the solution is unique. Furthermore, the solution has a unique extension forward or backward in time, either indefinitely or until $\boldsymbol{\varphi}(t)$ reaches the boundary of $\mathcal{D}$.

Corollary : *Different trajectories never intersect!*

1.1.4 Evolution of Phase Space Volumes

In general we are interested in finding integral curves $\boldsymbol{\varphi}(t)$. However, consider for the moment a collection of points in phase space comprising a region $\mathcal{R}$. As the dynamical system evolves, this region will also evolve, so that $\mathcal{R} = \mathcal{R}(t)$. We now ask: how does the volume of $\mathcal{R}(t)$,

$$\mathrm{vol}\big[\mathcal{R}(t)\big] = \int\limits_{\mathcal{R}(t)} d\mu \ , \tag{1.6}$$

where $d\mu = d\varphi_1 d\varphi_2 \cdots d\varphi_N$ is the phase space measure, change with time. We have, explicitly,

$$\begin{aligned}
\mathrm{vol}\big[\mathcal{R}(t+dt)\big] &= \int\limits_{\mathcal{R}(t+dt)} d\mu \\
&= \int\limits_{\mathcal{R}(t)} d\mu \left\| \frac{\partial \varphi_i(t+dt)}{\partial \varphi_j(t)} \right\| \\
&= \int\limits_{\mathcal{R}(t)} d\mu \Big\{ 1 + \boldsymbol{\nabla}\cdot\boldsymbol{V}\, dt + \mathcal{O}\big((dt)^2\big) \Big\} \ ,
\end{aligned} \tag{1.7}$$

since

$$\frac{\partial \varphi_i(t+dt)}{\partial \varphi_j(t)} = \delta_{ij} + \left.\frac{\partial V_i}{\partial \varphi_j}\right|_{\boldsymbol{\varphi}(t)} dt + \mathcal{O}\big((dt)^2\big) \ , \tag{1.8}$$

and, using $\ln\det M = \mathrm{Tr}\ln M$,

$$\det(1+\epsilon A) = 1 + \epsilon\,\mathrm{Tr}A + \mathcal{O}(\epsilon^2) \ . \tag{1.9}$$

Thus,

$$\frac{d}{dt}\,\mathrm{vol}\big[\mathcal{R}(t)\big] = \int\limits_{\mathcal{R}(t)} d\mu\, \boldsymbol{\nabla}\cdot\boldsymbol{V} \tag{1.10}$$

$$= \int\limits_{\partial\mathcal{R}(t)} d\Sigma\, \hat{\boldsymbol{n}}\cdot\boldsymbol{V} \ , \tag{1.11}$$

where in the last line we have used Stokes' theorem to convert the volume integral over $\mathcal{R}$ to a surface integral over its boundary $\partial\mathcal{R}$.

1.1.5 Lyapunov Characteristic Exponents

Suppose $\boldsymbol{\varphi}(t)$ is an integral curve – *i.e.* a solution of $\dot{\boldsymbol{\varphi}} = \boldsymbol{V}(\boldsymbol{\varphi})$. We now ask: how do nearby trajectories behave? Do they always remain close to $\boldsymbol{\varphi}(t)$ for all t? To answer this, we write $\widetilde{\boldsymbol{\varphi}}(t) \equiv \boldsymbol{\varphi}(t) + \boldsymbol{\eta}(t)$, in which case

$$\frac{d}{dt}\,\eta_i(t) = M_{ij}(t)\,\eta_j(t) + \mathcal{O}\big(\eta^2\big) \ , \tag{1.12}$$

where

$$M_{ij}(t) = \left.\frac{\partial V_i}{\partial \varphi_j}\right|_{\boldsymbol{\varphi}(t)} \ . \tag{1.13}$$

The solution, valid to first order in $\delta\boldsymbol{\varphi}$, is

$$\eta_i(t) = Q_{ij}(t, t_0)\, \eta_j(t_0) \ , \tag{1.14}$$

where the matrix $Q(t, t_0)$ is given by the *path ordered exponential,*

$$Q(t, t_0) = \mathcal{P} \exp\left\{ \int\limits_{t_0}^{t} dt'\, M(t') \right\} \tag{1.15}$$

$$\equiv \lim_{N\to\infty} \Big(1 + \frac{\Delta t}{N}\, M(t_{N-1})\Big) \cdots \Big(1 + \frac{\Delta t}{N}\, M(t_1)\Big) \Big(1 + \frac{\Delta t}{N}\, M(t_0)\Big) \ , \tag{1.16}$$

with $\Delta t = t - t_0$ and $t_j = t_0 + (j/N)\Delta t$. $\mathcal{P}$ is the *path ordering operator*, which places earlier times to the right:

$$\mathcal{P} A(t)\, B(t') = \begin{cases} A(t)\, B(t') & \text{if } t > t' \\ \\ B(t')\, A(t) & \text{if } t < t' \ . \end{cases} \tag{1.17}$$

The distinction is important if $\big[A(t), B(t')\big] \neq 0$. Note that Q satisfies the composition property,

$$Q(t, t_0) = Q(t, t_1)\, Q(t_1, t_0) \tag{1.18}$$

for any $t_1 \in [t_0, t]$. When M is time-independent, as in the case of a *fixed point* where $\boldsymbol{V}(\boldsymbol{\varphi}^*) = 0$, the path ordered exponential reduces to the ordinary exponential, and $Q(t, t_0) = \exp\big(M(t - t_0)\big)$.

Generally it is impossible to analytically compute path-ordered exponentials. However, the following example may be instructive. Suppose

$$M(t) = \begin{cases} M_1 & \text{if } t/T \in \big[2j, 2j+1\big] \\ \\ M_2 & \text{if } t/T \in \big[2j+1, 2j+2\big] \ , \end{cases} \tag{1.19}$$

for all integer j. $M(t)$ is a 'matrix-valued square wave', with period $2T$. Then, integrating over one period, from $t = 0$ to $t = 2T$, we have

$$A \equiv \ \exp\left\{ \int\limits_{0}^{2T} dt\, M(t) \right\} = e^{(M_1 + M_2)\, T} \tag{1.20}$$

$$A_{\mathcal{P}} \equiv \mathcal{P} \exp\left\{ \int\limits_{0}^{2T} dt\, M(t) \right\} = e^{M_2\, T}\, e^{M_1\, T} \ . \tag{1.21}$$

In general, $A \neq A_{\mathcal{P}}$, so the path ordering has a nontrivial effect[2].

The Lyapunov exponents are defined in the following manner. Let $\hat{\boldsymbol{e}}$ be an N-dimensional unit vector. Define

$$\Lambda(\boldsymbol{\varphi}_0, \hat{\boldsymbol{e}}) \equiv \lim_{t\to\infty} \lim_{b\to 0} \frac{1}{t - t_0} \ln \left(\frac{\big\|\boldsymbol{\eta}(t)\big\|}{\big\|\boldsymbol{\eta}(t_0)\big\|} \right)_{\boldsymbol{\eta}(t_0) = b\,\hat{\boldsymbol{e}}} , \tag{1.22}$$

where $\|\cdot\|$ denotes the Euclidean norm of a vector, and where $\boldsymbol{\varphi}_0 = \boldsymbol{\varphi}\big(t_0\big)$. A theorem due to Oseledec guarantees that there are N such values $\Lambda_i(\boldsymbol{\varphi}_0)$, depending on the choice of $\hat{\boldsymbol{e}}$, for a given $\boldsymbol{\varphi}_0$. Specifically, the theorem guarantees that the matrix

$$\hat{\mathcal{Q}} \equiv \big(Q^{\mathrm{t}} Q\big)^{1/(t-t_0)} \tag{1.23}$$

converges in the limit $t \to \infty$ for almost all $\boldsymbol{\varphi}_0$. The eigenvalues Λ_i correspond to the different eigenspaces of R. Oseledec's theorem (also called the 'multiplicative ergodic theorem') guarantees that the eigenspaces of Q either grow ($\Lambda_i > 1$) or shrink ($\Lambda_i < 1$) *exponentially* fast. That is, the norm any vector lying in the i^{th} eigenspace of Q will behave as $\exp\big(\Lambda_i\,(t - t_0)\big)$, for $t \to \infty$.

Note that while $\hat{\mathcal{Q}} = \hat{\mathcal{Q}}^{\mathrm{t}}$ is symmetric by construction, Q is simply a general real-valued $N \times N$ matrix. The left and right eigenvectors of a matrix $M \in \mathrm{GL}(N, \mathbf{R})$ will in general be different. The set of eigenvalues λ_α is, however, common to both sets of eigenvectors. Let $\{\psi_\alpha\}$ be the right eigenvectors and $\{\chi^*_\alpha\}$ the left eigenvectors, such that

$$M_{ij}\,\psi_{\alpha,j} = \lambda_\alpha\,\psi_{\alpha,i} \tag{1.24}$$

$$\chi^*_{\alpha,i}\,M_{ij} = \lambda_\alpha\,\chi^*_{\alpha,j}\ . \tag{1.25}$$

We can always choose the left and right eigenvectors to be orthonormal, *viz.*

$$\big\langle \chi_\alpha \big| \psi_\beta \big\rangle = \chi^*_{\alpha,i}\,\psi_{\beta,j} = \delta_{\alpha\beta}\ . \tag{1.26}$$

Indeed, we can define the matrix $S_{i\alpha} = \psi_{\alpha,i}$, in which case $S^{-1}_{\alpha j} = \chi^*_{\alpha,j}$, and

$$S^{-1}\,M\,S = \mathrm{diag}\big(\lambda_1, \ldots, \lambda_N\big)\ . \tag{1.27}$$

The matrix M can always be decomposed into its eigenvectors, as

$$M_{ij} = \sum_\alpha \lambda_\alpha\,\psi_{\alpha,i}\,\chi^*_{\alpha,j}\ . \tag{1.28}$$

If we expand $\boldsymbol{u}$ in terms of the right eigenvectors,

$$\boldsymbol{\eta}(t) = \sum_\beta C_\beta(t)\,\boldsymbol{\psi}_\beta(t)\ , \tag{1.29}$$

[2]If $\big[M_1, M_2\big] = 0$ then $A = A_{\mathcal{P}}$.

then upon taking the inner product with $\boldsymbol{\chi}_\alpha$, we find that C_α obeys

$$\dot{C}_\alpha + \langle \chi_\alpha | \dot{\psi}_\beta \rangle \, C_\beta = \lambda_\alpha \, C_\alpha \ . \tag{1.30}$$

If $\dot{\boldsymbol{\psi}}_\beta = 0$, *e.g.* if M is time-independent, then $C_\alpha(t) = C_\alpha(0)\, e^{\lambda_\alpha t}$, and

$$\eta_i(t) = \sum_\alpha \overbrace{\sum_j \eta_j(0)\, \chi^*_{\alpha,j}}^{C_\alpha(0)} \ e^{\lambda_\alpha t}\, \psi_{\alpha,i} \ . \tag{1.31}$$

Thus, the component of $\boldsymbol{\eta}(t)$ along $\boldsymbol{\psi}_\alpha$ increases exponentially with time if $\mathrm{Re}(\lambda_\alpha) > 0$, and decreases exponentially if $\mathrm{Re}(\lambda_\alpha) < 0$.

1.1.6 Linear Differential Equations

A homogeneous linear N^{th} order ODE,

$$\frac{d^N x}{dt^N} + c_{N-1}\,\frac{d^{N-1}x}{dt^{N-1}} + \ldots + c_1\,\frac{dx}{dt} + c_0 = 0 \tag{1.32}$$

may be written in matrix form, as

$$\frac{d}{dt}\begin{pmatrix} \varphi_1 \\ \varphi_2 \\ \vdots \\ \varphi_N \end{pmatrix} = \overbrace{\begin{pmatrix} 0 & 1 & 0 & \cdots & 0 \\ 0 & 0 & 1 & \cdots & 0 \\ \vdots & \vdots & \vdots & & \vdots \\ -c_0 & -c_1 & -c_2 & \cdots & -c_{N-1} \end{pmatrix}}^{M} \begin{pmatrix} \varphi_1 \\ \varphi_2 \\ \vdots \\ \varphi_N \end{pmatrix} \ . \tag{1.33}$$

Thus,

$$\dot{\boldsymbol{\varphi}} = M\boldsymbol{\varphi} \ , \tag{1.34}$$

and if the coefficients c_k are time-independent, *i.e.* the ODE is *autonomous*, the solution is obtained by exponentiating the constant matrix Q:

$$\boldsymbol{\varphi}(t) = \exp(Mt)\, \boldsymbol{\varphi}(0) \ ; \tag{1.35}$$

the exponential of a matrix may be given meaning by its Taylor series expansion. If the ODE is not autonomous, then $M = M(t)$ is time-dependent, and the solution is given by the path-ordered exponential,

$$\boldsymbol{\varphi}(t) = \mathcal{P} \exp\left\{ \int_0^t dt'\, M(t') \right\} \boldsymbol{\varphi}(0) \ , \tag{1.36}$$

As defined, the equation $\dot{\boldsymbol{\varphi}} = \boldsymbol{V}(\boldsymbol{\varphi})$ is autonomous, since g_t depends only on t and on no other time variable. However, by extending the phase space from $\mathcal{M}$ to $\mathbf{R} \times \mathcal{M}$, which is of dimension $(N+1)$, one can describe arbitrary time-dependent ODEs.

1.2 $N = 1$ Systems

We now study phase flows in a one-dimensional phase space, governed by the equation

$$\frac{du}{dt} = f(u) \ . \tag{1.37}$$

Again, the equation $\dot{u} = h(u,t)$ is first order, but not autonomous, and it corresponds to the $N = 2$ system,

$$\frac{d}{dt}\begin{pmatrix} u \\ t \end{pmatrix} = \begin{pmatrix} h(u,t) \\ 1 \end{pmatrix} \ . \tag{1.38}$$

The equation 1.37 is easily integrated:

$$\frac{du}{f(u)} = dt \qquad \Longrightarrow \qquad \boxed{t - t_0 = \int\limits_{u_0}^{u} \frac{du'}{f(u')}} \ . \tag{1.39}$$

This gives $t(u)$; we must then invert this relationship to obtain $u(t)$.

Example : Suppose $f(u) = a - bu$, with a and b constant. Then

$$dt = \frac{du}{a - bu} = -b^{-1}\, d\ln(a - bu) \tag{1.40}$$

whence

$$t = \frac{1}{b}\ln\left(\frac{a - b\,u(0)}{a - b\,u(t)}\right) \quad \Longrightarrow \quad u(t) = \frac{a}{b} + \left(u(0) - \frac{a}{b}\right)\exp(-bt) \ . \tag{1.41}$$

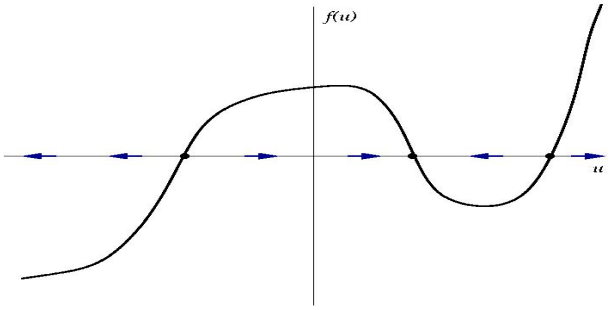

Figure 1.2: Phase flow for an $N = 1$ system.

Even if one cannot analytically obtain $u(t)$, the behavior is very simple, and easily obtained by graphical analysis. Sketch the function $f(u)$. Then note that

$$\dot{u} = f(u) \quad \Longrightarrow \quad \begin{cases} f(u) > 0 & \dot{u} > 0 \quad \Rightarrow \quad \text{move to right} \\ f(u) < 0 & \dot{u} < 0 \quad \Rightarrow \quad \text{move to left} \\ f(u) = 0 & \dot{u} = 0 \quad \Rightarrow \quad \text{fixed point} \end{cases} \tag{1.42}$$

The behavior of $N = 1$ systems is particularly simple: $u(t)$ flows to the first stable fixed point encountered, where it then (after a logarithmically infinite time) stops. The motion is monotonic – the velocity $\dot{u}$ never changes sign. Thus, *oscillations never occur for* $N = 1$ *phase flows.*[3]

1.2.1 Classification of Fixed Points ($N = 1$)

A *fixed point* u^* satisfies $f(u^*) = 0$. Generically, $f'(u^*) \neq 0$ at a fixed point.[4] Suppose $f'(u^*) < 0$. Then to the left of the fixed point, the function $f(u < u^*)$ is positive, and the flow is to the right, *i.e.* toward u^*. To the right of the fixed point, the function $f(u > u^*)$ is negative, and the flow is to the left, *i.e.* again toward u^*. Thus, when $f'(u^*) < 0$ the fixed point is said to be *stable*, since the flow in the vicinity of u^* is to u^*. Conversely, when $f'(u^*) > 0$, the flow is always away from u^*, and the fixed point is then said to be *unstable*. Indeed, if we linearize about the fixed point, and let $\epsilon \equiv u - u^*$, then

$$\dot{\epsilon} = f'(u^*)\,\epsilon + \tfrac{1}{2}\,f''(u^*)\,\epsilon^2 + \mathcal{O}(\epsilon^3)\ , \tag{1.43}$$

and dropping all terms past the first on the RHS gives

$$\epsilon(t) = \exp\Big[f'(u^*)\,t\Big]\,\epsilon(0)\ . \tag{1.44}$$

The deviation decreases exponentially for $f'(u^*) < 0$ and increases exponentially for $f(u^*) > 0$. Note that

$$t(\epsilon) = \frac{1}{f'(u^*)}\,\ln\left(\frac{\epsilon}{\epsilon(0)}\right)\ , \tag{1.45}$$

so the approach to a stable fixed point takes a logarithmically infinite time. For the unstable case, the deviation grows exponentially, until eventually the linearization itself fails.

1.2.2 Logistic Equation

This model for population growth was first proposed by Verhulst in 1838. Let N denote the population in question. The dynamics are modeled by the first order ODE,

$$\frac{dN}{dt} = rN\Big(1 - \frac{N}{K}\Big)\ , \tag{1.46}$$

where N, r, and K are all positive. For $N \ll K$ the growth rate is r, but as N increases a quadratic nonlinearity kicks in and the rate vanishes for $N = K$ and is negative for $N > K$. The nonlinearity models the effects of competition between the organisms for food, shelter, or other resources. Or maybe they crap all over each other and get sick. Whatever. There are two fixed points, one at $N^* = 0$, which is unstable ($f'(0) = r > 0$). The other, at

[3] When I say 'never' I mean 'sometimes' – see the section 1.4.

[4] The system $f(u^*) = 0$ and $f'(u^*) = 0$ is overdetermined, with two equations for the single variable u^*.

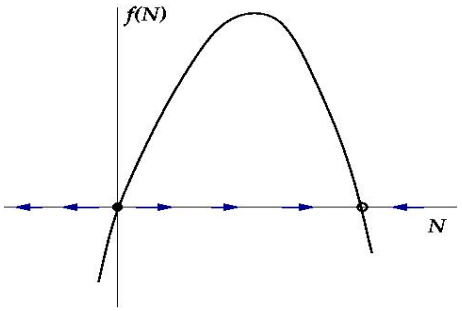

Figure 1.3: Flow diagram for the logistic equation.

$N^* = K$, is stable ($f'(K) = -r$). The equation is adimensionalized by defining $\nu = N/K$ and $s = rt$, whence

$$\dot{\nu} = \nu(1-\nu) \ . \tag{1.47}$$

Integrating,

$$\frac{d\nu}{\nu(1-\nu)} = d\ln\Big(\frac{\nu}{1-\nu}\Big) = ds \quad \Longrightarrow \quad \boxed{\nu(s) = \frac{\nu_0}{\nu_0 + \big(1-\nu_0\big)\exp(-s)}} \ . \tag{1.48}$$

As $s \to \infty$, $\nu(s) = 1 - \big(\nu_0^{-1} - 1\big)\, e^{-s} + \mathcal{O}(e^{-2s})$, and the relaxation to equilibrium ($\nu^* = 1$) is exponential, as usual.

Another application of this model is to a simple autocatalytic reaction, such as

$$A + X \rightleftharpoons 2X \ , \tag{1.49}$$

i.e. X catalyses the reaction $A \longrightarrow X$. Assuming a fixed concentration of A, we have

$$\dot{x} = \kappa_+ \, a \, x - \kappa_- \, x^2 \ , \tag{1.50}$$

where x is the concentration of X, and $\kappa_\pm$ are the forward and backward reaction rates.

1.2.3 Singular $f(u)$

Suppose that in the vicinity of a fixed point we have $f(u) = A\,\big|u - u^*\big|^\alpha$, with $A > 0$. The fixed point $u = u^*$ is now *half-stable* – the flow from the left is toward u^* but from the right is away from u^*. Let's analyze the flow on either side of u^*.

$\underline{u < u^*}$: Let $\epsilon = u^* - u$. Then

$$\dot{\epsilon} = -A\,\epsilon^\alpha \quad \Longrightarrow \quad \frac{\epsilon^{1-\alpha}}{1-\alpha} = \frac{\epsilon_0^{1-\alpha}}{1-\alpha} - At \ , \tag{1.51}$$

hence

$$\epsilon(t) = \Big[1 + (\alpha-1)A\,\epsilon_0^{\alpha-1}\,t\Big]^{\frac{1}{1-\alpha}} \ . \tag{1.52}$$

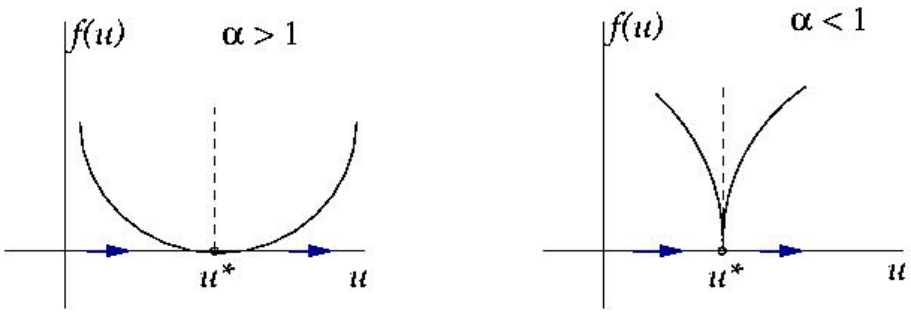

Figure 1.4: $f(u) = A\left|u - u^*\right|^\alpha$, for $\alpha > 1$ and $\alpha < 1$.

This, for $\alpha < 1$ the fixed point $\epsilon = 0$ is reached in a finite time: $\epsilon(t_c) = 0$, with

$$t_c = \frac{\epsilon_0^{1-\alpha}}{(1-\alpha)\,A} \ . \tag{1.53}$$

For $\alpha > 1$, we have $\lim_{t\to\infty} \epsilon(t) = 0$, but $\epsilon(t) > 0 \ \forall \ t < \infty$.

$\underline{u > u^*}$: Let $\epsilon = u - u^*$. Then $\dot\epsilon = A\,\epsilon^\alpha$, and

$$\epsilon(t) = \Big[1 + (1-\alpha)A\,\epsilon_0^{\alpha-1}\,t\Big]^{\frac{1}{1-\alpha}} \ . \tag{1.54}$$

For $\alpha < 1$, $\epsilon(t)$ escapes to $\epsilon = \infty$ only after an infinite time. For $\alpha > 1$, the escape to infinity takes a finite time: $\epsilon(t_c) = \infty$, with

$$t_c = \frac{\epsilon_0^{1-\alpha}}{(\alpha-1)\,A} \ . \tag{1.55}$$

In both cases, higher order terms in the (nonanalytic) expansion of $f(u)$ about $u = u^*$ will eventually come into play.

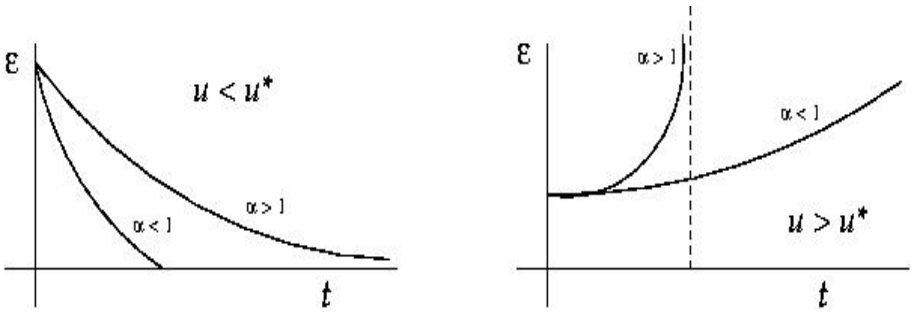

Figure 1.5: Solution to $\dot\epsilon = \mp A\,\epsilon^\alpha$.

1.2.4 Non-autonomous ODEs

Non-autonomous ODEs of the form $\dot{u} = h(u,t)$ are in general impossible to solve by quadratures. One can always go to the computer, but it is worth noting that in the *separable* case, $h(u,t) = f(u)\,g(t)$, one can obtain the solution

$$\frac{du}{f(u)} = g(t)\,dt \quad \Longrightarrow \quad \boxed{\int\limits_{u_0}^{u} \frac{du'}{f(u')} = \int\limits_{0}^{t} dt'\,g(t')} \;, \tag{1.56}$$

which implicitly gives $u(t)$. Note that $\dot{u}$ may now change sign, and $u(t)$ may even oscillate. For an explicit example, consider the equation

$$\dot{u} = A\,(u+1)\,\sin(\beta t) \;, \tag{1.57}$$

the solution of which is

$$u(t) = -1 + \big(u_0 + 1\big)\,\exp\left\{\frac{A}{\beta}\,\big[1 - \cos(\beta t)\big]\right\} . \tag{1.58}$$

In general, the non-autonomous case defies analytic solution. Many have been studied, such as the Riccati equation,

$$\frac{du}{dt} = P(t)u^2 + Q(t)u + R(t) \;. \tag{1.59}$$

Riccati equations have the special and remarkable property that one can generate *all* solutions (*i.e.* with arbitrary boundary condition $u(0) = u_0$) from *any* given solution (*i.e.* with any boundary condition).

1.3 Bifurcations

1.3.1 Saddle-node bifurcation

We remarked above how $f'(u)$ is in general nonzero when $f(u)$ itself vanishes, since two equations in a single unknown is an overdetermined set. However, consider the function $F(x,\alpha)$, where α is a control parameter. If we demand $F(x,\alpha) = 0$ and $\partial_x F(x,\alpha) = 0$, we have two equations in two unknowns, and in general there will be a zero-dimensional solution set consisting of points $(x_{\rm c}, \alpha_{\rm c})$. The situation is depicted in Fig. 1.6.

Let's expand $F(x,\alpha)$ in the vicinity of such a point $(x_{\rm c},\alpha_{\rm c})$:

$$\begin{aligned} F(x,\alpha) &= F(x_{\rm c},\alpha_{\rm c}) + \frac{\partial F}{\partial x}\bigg|_{(x_{\rm c},\alpha_{\rm c})}(x - x_{\rm c}) + \frac{\partial F}{\partial \alpha}\bigg|_{(x_{\rm c},\alpha_{\rm c})}(\alpha - \alpha_{\rm c}) + \frac{1}{2}\,\frac{\partial^2 F}{\partial x^2}\bigg|_{(x_{\rm c},\alpha_{\rm c})}(x - x_{\rm c})^2 \\ &\qquad + \frac{\partial^2 F}{\partial x\,\partial \alpha}\bigg|_{(x_{\rm c},\alpha_{\rm c})}(x - x_{\rm c})\,(\alpha - \alpha_{\rm c}) + \frac{1}{2}\,\frac{\partial^2 F}{\partial \alpha^2}\bigg|_{(x_{\rm c},\alpha_{\rm c})}(\alpha - \alpha_{\rm c})^2 + \ldots \qquad (1.60) \\ &= A\,(\alpha - \alpha_{\rm c}) + B\,(x - x_{\rm c})^2 + \ldots \;, \qquad (1.61) \end{aligned}$$

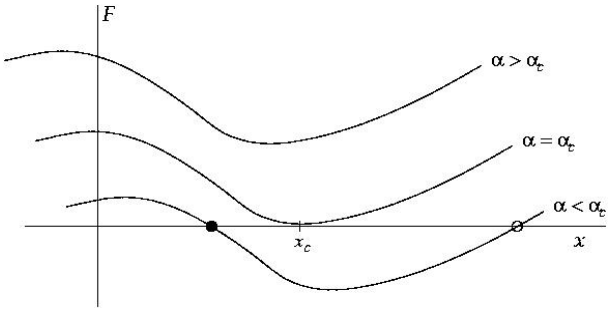

Figure 1.6: Evolution of $F(x, \alpha)$ as a function of the control parameter α.

where we keep terms of lowest order in the deviations δu and δr. If we now rescale $u \equiv \sqrt{B/A}\ (x - x_{\rm c})$, $r \equiv \alpha - \alpha_{\rm c}$, and $\tau = \sqrt{AB}\ t$, we have, neglecting the higher order terms, we obtain the 'normal form' of the saddle-node bifurcation,

$$\frac{du}{d\tau} = r + u^2 \ . \tag{1.62}$$

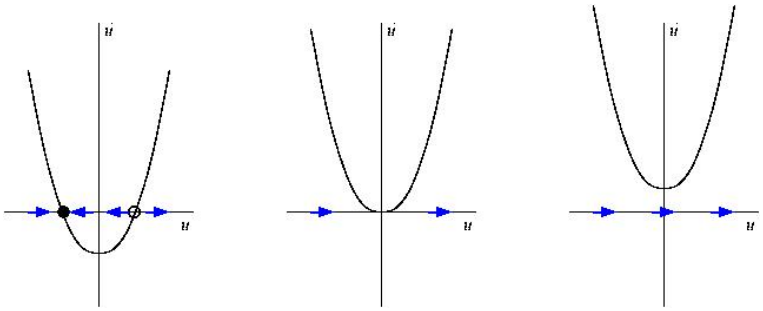

Figure 1.7: The saddle-node bifurcation.

The evolution of the flow is depicted in Fig. 1.7. For $r < 0$ there are two fixed points – one stable ($u^* = -\sqrt{-r}$) and one unstable ($u = +\sqrt{-r}$). At $r = 0$ these two nodes coalesce and annihilate each other. (The point $u^* = 0$ is half-stable precisely at $r = 0$.) For $r > 0$ there are no longer any fixed points in the vicinity of $u = 0$. In Fig. 1.8 we show the flow in the extended (r, u) plane. The unstable and stable nodes annihilate at $r = 0$.

1.3.2 Transcritical bifurcation

Another situation which arises frequently is the *transcritical bifurcation*. Consider the equation $\dot{x} = f(x)$ in the vicinity of a fixed point x^*.

$$\frac{dx}{dt} = f'(x^*)\,(x - x^*) + \tfrac{1}{2}\,f''(x^*)(x - x^*)^2 + \ldots \ . \tag{1.63}$$

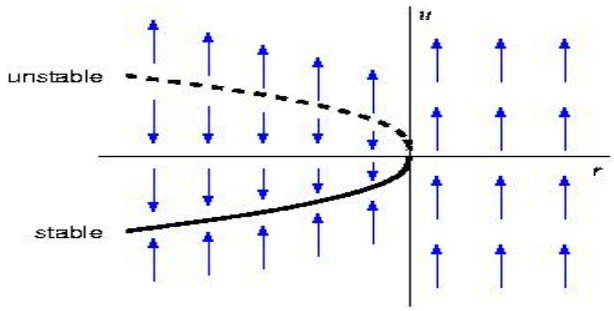

Figure 1.8: Flow diagram in (r, u) space for the saddle-node bifurcation.

We rescale $u \equiv \beta\,(x - x^*)$ with $\beta = -\frac{1}{2}\,f''(x^*)$ and define $r \equiv f'(x^*)$ as the control parameter, to obtain, to order u^2,

$$\frac{du}{dt} = ru - u^2 \ . \tag{1.64}$$

Note that the sign of the u^2 term can be reversed relative to the others by sending $u \to -u$ and $r \to -r$.

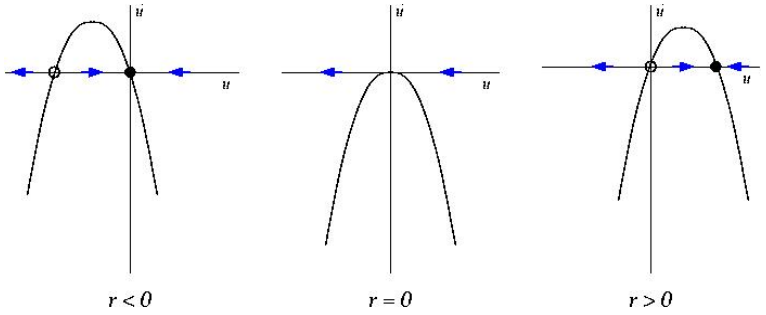

Figure 1.9: The transcritical bifurcation $\dot{u} = ru - u^2$.

What happens in the transcritical bifurcation is an exchange of stability of the fixed points at $u^* = 0$ and $u^* = r$ as r passes through zero. This is depicted graphically in figs. 1.9 and 1.10.

Consider a crude model of a laser threshold. Let n be the number of photons in the laser cavity, and N the number of excited atoms in the cavity. The dynamics of the laser are approximated by the equations

$$\dot{n} = GNn - kn \tag{1.65}$$

$$N = N_0 - \alpha n \ . \tag{1.66}$$

Here G is the gain coefficient and k the photon decay rate. N_0 is the pump strength, and α is a numerical factor. The first equation tells us that the number of photons in the cavity grows with a rate $GN - k$; gain is proportional to the number of excited atoms, and the loss rate is a constant cavity-dependent quantity (typically through the ends, which are

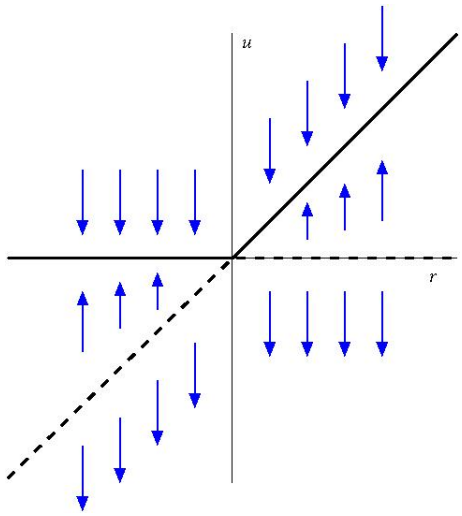

Figure 1.10: Extended phase space (r, u) flow diagram for the transcritical bifurcation.

semi-transparent). The second equation says that the number of excited atoms is equal to the pump strength minus a term proportional to the number of photons (since the presence of a photon means an excited atom has decayed). Putting them together,

$$\dot{n} = (GN_0 - k)\, n - \alpha G n^2 \ , \tag{1.67}$$

which exhibits a transcritical bifurcation at pump strength $N_0 = G/k$. For $N_0 < G/k$ the system acts as a lamp; for $N_0 > G/k$ the system acts as a laser.

1.3.3 Pitchfork bifurcation

The pitchfork bifurcation is commonly encountered in systems in which there is an overall parity symmetry ($u \to -u$). There are two classes of pitchfork - supercritical and subcritical. The normal form of the supercritical bifurcation is

$$\dot{u} = ru - u^3 \ , \tag{1.68}$$

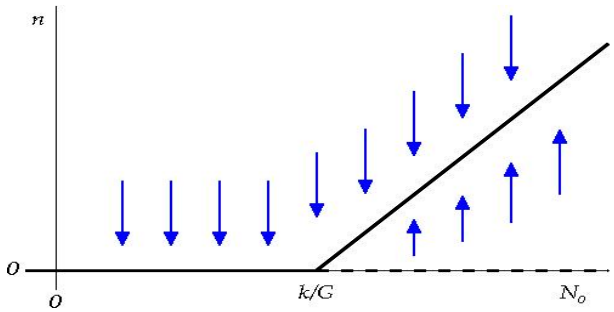

Figure 1.11: Transcritical bifurcation in a model of a laser.

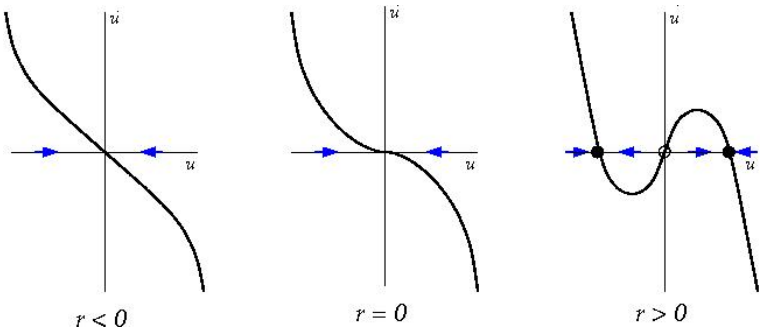

Figure 1.12: Pitchfork bifurcation $\dot{u} = ru - u^3$.

which has fixed points at $u^* = 0$ and $u^* = \pm\sqrt{r}$. Thus, the situation is as depicted in Fig. 1.12. For $r < 0$ there is a single stable fixed point at $u^* = 0$. For $r > 0$, $u^* = 0$ is unstable, and flanked by two stable fixed points at $u^* = \pm\sqrt{r}$. If we send $u \to -u$, $r \to -r$, and $t \to -t$, we obtain the *subcritical pitchfork*, depicted in Fig. 1.13. The fixed point structure in both cases is shown in Fig. 1.14.

1.3.4 Imperfect bifurcation

The imperfect bifurcation occurs when a symmetry-breaking term is added to the pitchfork. The normal form contains two control parameters:

$$\dot{u} = h + ru - u^3 \ . \tag{1.69}$$

Here, the constant h breaks the parity symmetry if $u \to -u$. This equation arises from a crude model of magnetization dynamics. Let M be the magnetization of a sample, and $F(M)$ the free energy. Assuming M is small, we can expand $F(M)$ as

$$F(M) = -HM + \tfrac{1}{2}aM^2 + \tfrac{1}{4}bM^4 + \dots \ , \tag{1.70}$$

where H is the external magnetic field, and a and b are temperature-dependent constants. This is called the *Landau expansion* of the free energy. We assume $b > 0$ in order that the

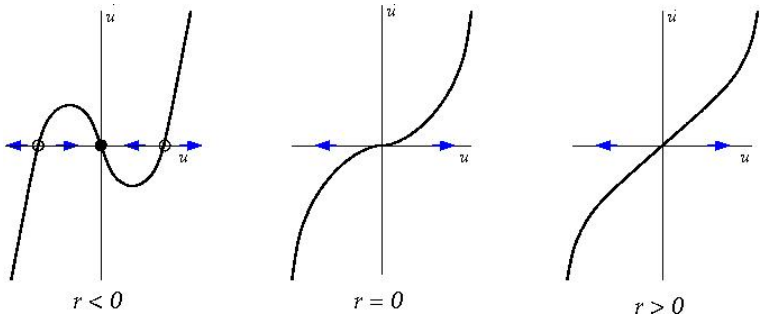

Figure 1.13: Pitchfork bifurcation $\dot{u} = ru + u^3$.

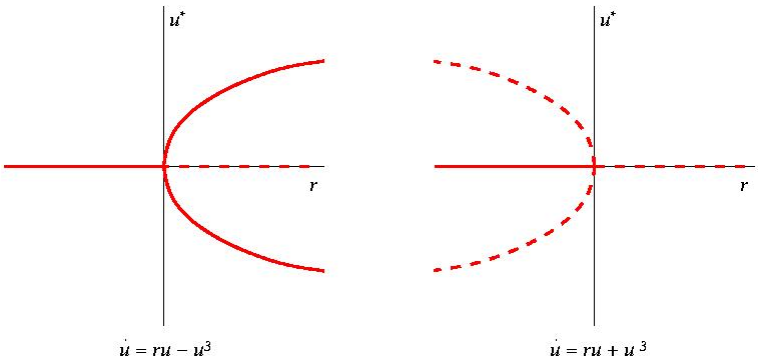

Figure 1.14: Fixed points and their stabilities for the supercritical (left) and subcritical (right) pitchfork bifurcations. Solid lines are for stable fixed points; dashed lines are unstable fixed points.

minimum of $F(M)$ not lie at infinity. The dynamics of $M(t)$ are modeled by

$$\frac{dM}{dt} = -\Gamma \, \frac{\partial F}{\partial M} \ , \tag{1.71}$$

with $\Gamma > 0$. Thus, the magnetization evolves toward a local minimum in the free energy. Note that the free energy is a decreasing function of time:

$$\frac{dF}{dt} = \frac{\partial F}{\partial M}\,\frac{dM}{dt} = -\Gamma\left(\frac{\partial F}{\partial M}\right)^2 \ . \tag{1.72}$$

By rescaling $M \equiv \alpha u$ with $\alpha = (b\,\Gamma)^{-1/2}$ and defining $r \equiv -(\Gamma/b)^{1/2}$ and $h \equiv (\Gamma^3\,b)^{1/2}\,H$, we obtain the normal form

$$\dot u = h + ru - u^3 = -\frac{\partial f}{\partial u} \tag{1.73}$$

$$f(u) = -\tfrac{1}{2}ru^2 + \tfrac{1}{4}u^4 - hu \ . \tag{1.74}$$

Here, $f(u)$ is a scaled version of the free energy.

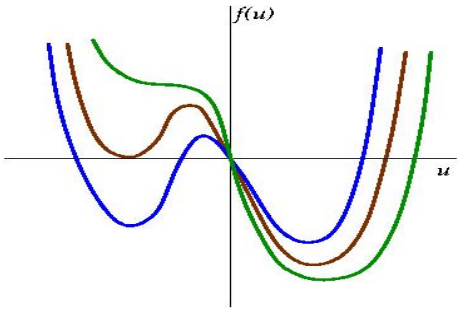

Figure 1.15: Scaled free energy $f(u) = -\frac{1}{2}ru^2 + \frac{1}{4}u^4 - hu$. Green curve: $h = h_{\rm c}(r) = \frac{2}{3\sqrt{3}}\,r^{3/2}$. Brown curve: $h = \frac{\sqrt{2}}{3\sqrt{3}}\,r^{3/2}$. Blue curve: $h < \frac{\sqrt{2}}{3\sqrt{3}}\,r^{3/2}$.

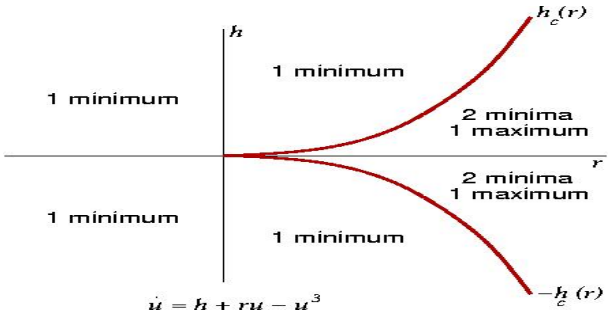

Figure 1.16: Phase diagram for the imperfect bifurcation $\dot{u} = hu + ru - u^3$.

Fixed points satisfy the equation

$$u^3 - ru - h = 0 \ , \tag{1.75}$$

and correspond to extrema in $f(u)$. By the fundamental theorem of algebra, this cubic polynomial may be uniquely factorized over the complex plane. Since the coefficients are real, the complex conjugate $\bar{u}$ satisfies the same equation as u, hence there are two possibilities for the roots: either (i) all three roots are real, or (ii) one root is real and the other two are a complex conjugate pair. Clearly for $r < 0$ we are in situation (ii), since $u^3 - ru$ is then monotonically increasing for $u \in \mathbf{R}$, and therefore takes the value h precisely once for u real. For $r > 0$, there is a region $h \in \big[-h_{\rm c}(r), h_{\rm c}(r) \big]$ over which there are three real roots. To find $h_{\rm c}(r)$, we demand $f''(u) = 0$ as well as $f'(u) = 0$, which says that two roots have merged, forming an inflection point. One easily finds $h_{\rm c}(r) = \frac{2}{3\sqrt{3}}\, r^{3/2}$.

Examples of the function $f(u)$ for $r > 0$ are shown in Fig. 1.15 for three different values of h. For $|h| < h_{\rm c}(r)$ there are three extrema satisfying $f'(u^*) = 0$: $u_1^* < u_2^* < 0 < u_3^*$, assuming (without loss of generality) that $h > 0$. Clearly u_1^* is a local minimum, u_2^* a local maximum, and u_3^* the global minimum of the function $f(u)$. The 'phase diagram' for this system, plotted in the (r, h) control parameter space, is shown in Fig. 1.16.

In Fig. 1.17 we plot the fixed points $u^*(r)$ for fixed h. A saddle-node bifurcation occurs at $r = r_{\rm c}(h) = \frac{3}{2^{2/3}}\, |h|^{2/3}$. For $h = 0$ this reduces to the supercritical pitchfork; for finite h

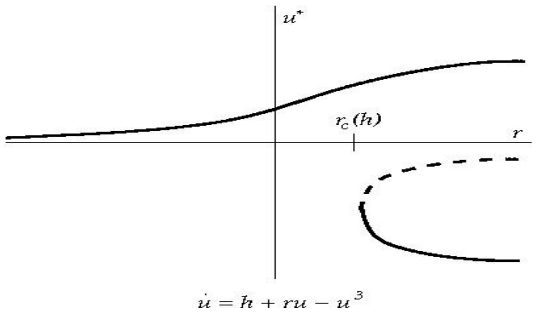

Figure 1.17: $u^*(r)$ at fixed h for the imperfect bifurcation. This is in a sense a deformed supercritical pitchfork.

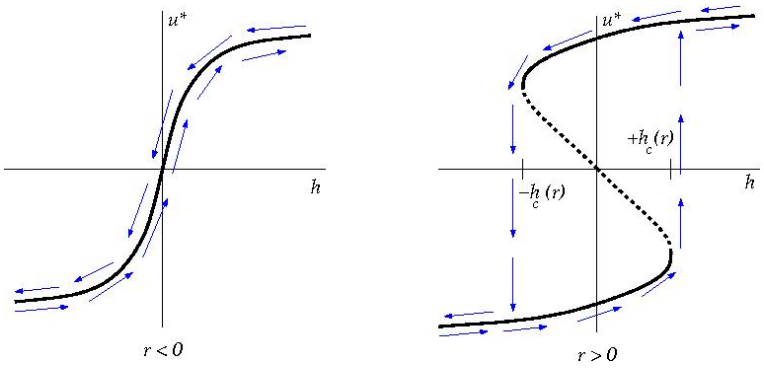

Figure 1.18: $u^*(h)$ at fixed r for the imperfect bifurcation. For $r < 0$ the behavior is completely reversible. For $r > 0$, a regime of irreversibility sets in between $-h_{\rm c}(r)$ and $+h_{\rm c}(r)$.

the pitchfork is deformed and even changed topologically. Finally, in Fig. 1.18 we show the behavior of $u^*(h)$ for fixed r. When $r < 0$ the curve retraces itself as h is ramped up and down, but for $r > 0$ the system exhibits hysteresis, *i.e.* there is an irreversible aspect to the behavior.

1.3.5 Lyapunov Functions

For a general dynamical system $\dot{\boldsymbol{\varphi}} = \boldsymbol{V}(\boldsymbol{\varphi})$, a *Lyapunov function* $L(\boldsymbol{\varphi})$ is a function which satisfies

$$\boldsymbol{\nabla} L(\boldsymbol{\varphi}) \cdot \boldsymbol{V}(\boldsymbol{\varphi}) \leq 0 \ . \tag{1.76}$$

There is no simple way to determine whether a Lyapunov function exists for a given dynamical system, or, if it does exist, what the Lyapunov function is. However, if a Lyapunov function can be found, then this severely limits the possible behavior of the system. This is because $L\big(\boldsymbol{\varphi}(t)\big)$ must be a monotonic function of time:

$$\frac{d}{dt}\, L\big(\boldsymbol{\varphi}(t)\big) = \boldsymbol{\nabla} L \cdot \frac{d\boldsymbol{\varphi}}{dt} = \boldsymbol{\nabla} L(\boldsymbol{\varphi}) \cdot \boldsymbol{V}(\boldsymbol{\varphi}) \leq 0 \ . \tag{1.77}$$

Thus, the system evolves toward a local minimum of the Lyapunov function. In general this means that oscillations are impossible in systems for which a Lyapunov function exists. In the above example, the free energy $F(M)$ itself is a Lyapunov function. Indeed, the dynamics $\dot{M} = -\Gamma F'(M)$ is explicitly constructed so as to make $F(M)$ a Lyapunov function.

1.4 Flows on the Circle

We had remarked that oscillations are impossible for the equation $\dot{u} = f(u)$ because the flow is to the first stable fixed point encountered. If there are no stable fixed points, the

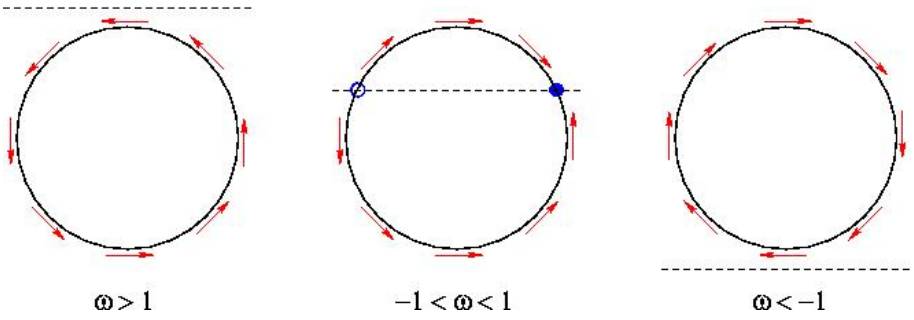

Figure 1.19: Flow for the nonuniform oscillator $\dot\theta = \omega - \sin\theta$ for three characteristic values of ω.

flow is unbounded. However, suppose phase space itself is bounded, *e.g.* a circle S^1 rather than the real line $\mathbf{R}$. Thus,

$$\dot\theta = f(\theta) \ , \tag{1.78}$$

with $f(\theta + 2\pi) = f(\theta)$. Now if there are no fixed points, $\theta(t)$ endlessly winds around the circle, and in this sense we can have oscillations.

A particularly common example is that of the nonuniform oscillator,

$$\dot\theta = \omega - \sin\theta \ , \tag{1.79}$$

which has applications to electronics, biology, classical mechanics, and condensed matter physics. (The general equation $\dot\theta = \omega - A\sin\theta$ may be rescaled to the above form.) Fixed points occur only for $\omega < 1$, for $\sin\theta = \omega$. To integrate, set $z = \exp(i\theta)$, in which case

$$\begin{aligned}\dot z &= -\tfrac{1}{2}(z^2 - 2i\omega z - 1) \\ &= -\tfrac{1}{2}(z - z_-)(z - z_+) \ ,\end{aligned} \tag{1.80}$$

where $\nu = \sqrt{1-\omega^2}$ and $z_\pm = i\omega \pm \nu$. Note that for $\omega^2 < 1$, ν is real, and $z(t \to \mp\infty) = z_\pm$. This equation can easily be integrated, yielding

$$z(t) = \frac{(z(0) - z_-)\, z_+ - (z(0) - z_+)\, z_- \, \exp(\nu t)}{(z(0) - z_-) - (z(0) - z_+)\, \exp(\nu t)} \ , \tag{1.81}$$

For $\omega^2 > 1$, the motion is periodic, with period

$$T = \int_0^{2\pi} \frac{d\theta}{|\omega| - \sin\theta} = \frac{2\pi}{\sqrt{\omega^2 - 1}} \ . \tag{1.82}$$

The situation is depicted in Fig. 1.19.

1.5 $N = 2$ Systems

The general form to be studied is

$$\frac{d}{dt}\begin{pmatrix} x \\ y \end{pmatrix} = \begin{pmatrix} V_x(x,y) \\ V_y(x,y) \end{pmatrix} \ . \tag{1.83}$$

Special cases include autonomous second order ODEs, *viz.*

$$\ddot{x} = f(x,\dot{x}) \qquad \Longrightarrow \qquad \frac{d}{dt}\begin{pmatrix} x \\ v \end{pmatrix} = \begin{pmatrix} v \\ f(x,v) \end{pmatrix} \ , \tag{1.84}$$

and Hamiltonian systems,

$$\frac{d}{dt}\begin{pmatrix} q \\ p \end{pmatrix} = \begin{pmatrix} \partial H/\partial p \\ \partial H/\partial q \end{pmatrix} \ . \tag{1.85}$$

Another example is that of the damped and driven harmonic oscillator,

$$\frac{d^2\phi}{ds^2} + \frac{1}{\beta}\frac{d\phi}{ds} + \sin\phi = j \ . \tag{1.86}$$

This is equivalent to a model of a resistively and capacitively shunted Josephson junction. Writing this as two first order equations,

$$\frac{d}{dt}\begin{pmatrix} \phi \\ \omega \end{pmatrix} = \begin{pmatrix} \omega \\ j - \sin\phi - \beta^{-1}\omega \end{pmatrix} \ , \tag{1.87}$$

where $\omega = \dot{\phi}$. Phase space is a cylinder, $\mathrm{S}^1 \times \mathbf{R}^1$. At a fixed point, both components of the vector field $\boldsymbol{V}(\phi,\omega)$ must vanish. This requires $\omega = 0$ and $j = \sin\phi$. Therefore, there are two fixed points for $|j| < 1$, one a saddle point and the other a stable spiral. For $|j| > 1$ there are no fixed points, and asymptotically the function $\phi(t)$ tends to a periodic *limit cycle* $\phi_{\rm LC}(t)$. The flow is sketched for two representative values of j in Fig. 1.20.

1.5.1 Classification of $N = 2$ Fixed Points

Suppose we have solved the fixed point equations $V_x(x^*,y^*) = 0$ and $V_y(x^*,y^*) = 0$. Let us now expand about the fixed point, writing

$$\dot{x} = \left.\frac{\partial V_x}{\partial x}\right|_{(x^*,y^*)} (x - x^*) + \left.\frac{\partial V_x}{\partial y}\right|_{(x^*,y^*)} (y - y^*) + \ldots \tag{1.88}$$

$$\dot{y} = \left.\frac{\partial V_y}{\partial x}\right|_{(x^*,y^*)} (x - x^*) + \left.\frac{\partial V_y}{\partial y}\right|_{(x^*,y^*)} (y - y^*) + \ldots \ . \tag{1.89}$$

We define

$$u_1 = x - x^* \qquad , \qquad u_2 = y - y^* \ , \tag{1.90}$$

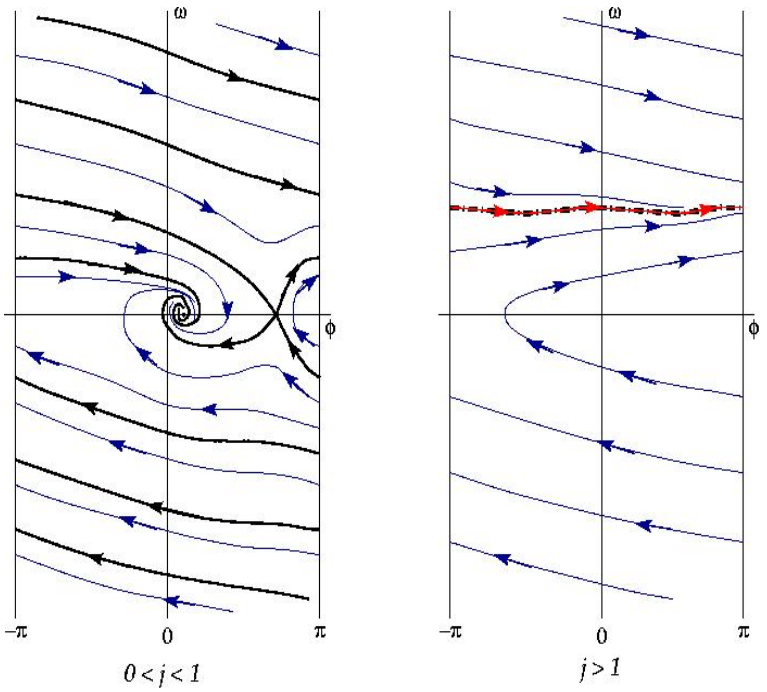

Figure 1.20: Phase flows for the equation $\ddot{\phi} + \beta^{-1}\dot{\phi} + \sin\phi = j$. Left panel: $0 < j < 1$; note the separatrix (in black), which flows into the stable and unstable fixed points. Right panel: $j > 1$. The red curve overlying the thick black dot-dash curve is a *limit cycle*.

which, to linear order, satisfy

$$\frac{d}{dt}\begin{pmatrix} u_1 \\ u_2 \end{pmatrix} = \overbrace{\begin{pmatrix} a & b \\ c & d \end{pmatrix}}^{M} \begin{pmatrix} u_1 \\ u_2 \end{pmatrix} + \mathcal{O}(u^2) \ . \tag{1.91}$$

The formal solution to $\dot{\boldsymbol{u}} = M\boldsymbol{u}$ is

$$\boldsymbol{u}(t) = \exp(Mt)\,\boldsymbol{u}(0) \ , \tag{1.92}$$

where $\exp(Mt) = \sum_{n=0}^{\infty} \frac{1}{n!}\,(Mt)^n$ is the exponential of the matrix Mt.

The eigenvalues are roots of the characteristic equation $P(\lambda) = 0$, where

$$\begin{aligned} P(\lambda) &= \det(\lambda\mathbf{1} - M) \\ &= \lambda^2 - T\lambda + D \ , \end{aligned} \tag{1.93}$$

with $T = a + d = \mathrm{Tr}(M)$ and $D = ad - bc = \det(M)$. The two eigenvalues are therefore

$$\lambda_\pm = \tfrac{1}{2}\Big(T \pm \sqrt{T^2 - 4D}\Big) \ . \tag{1.94}$$

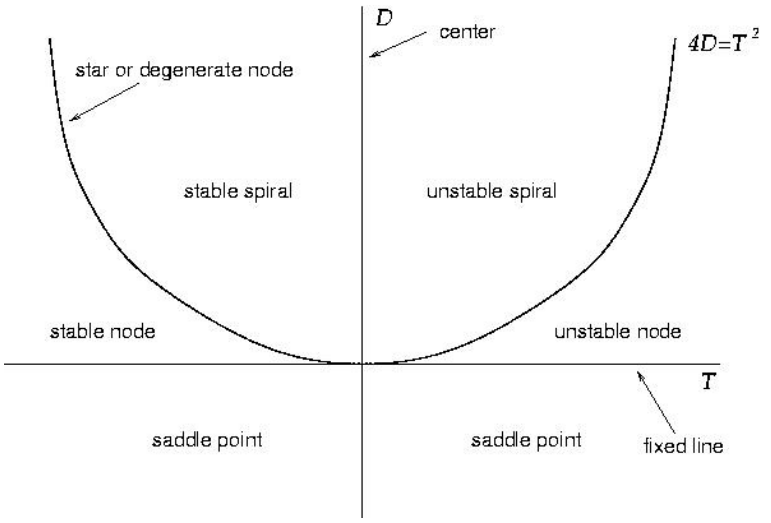

Figure 1.21: Complete classification of fixed points for the $N = 2$ system.

1.5.2 The Fixed Point Zoo

- **Saddles** : When $D < 0$, both eigenvalues are real; one is positive and one is negative, *i.e.* $\lambda_+ > 0$ and $\lambda_- < 0$. The right eigenvector $\boldsymbol{\psi}_-$ is thus the *stable direction* while $\boldsymbol{\psi}_+$ is the *unstable direction*. Going beyond the linear analysis, we define the *stable manifold* $\mathcal{Q}_{\rm s}(\boldsymbol{\varphi}^*)$ and the *unstable manifold* $\mathcal{Q}_{\rm u}(\boldsymbol{\varphi}^*)$ associated with the fixed point $\boldsymbol{\varphi}^*$ by

$$\mathcal{Q}_{\rm s}(\boldsymbol{\varphi}^*) \equiv \left\{ \boldsymbol{\varphi} \in \mathcal{M} \;\middle|\; \lim_{\tau\to\infty} g_\tau\, \boldsymbol{\varphi} = \boldsymbol{\varphi}^* \right\} \tag{1.95}$$

$$\mathcal{Q}_{\rm u}(\boldsymbol{\varphi}^*) \equiv \left\{ \boldsymbol{\varphi} \in \mathcal{M} \;\middle|\; \lim_{\tau\to-\infty} g_\tau\, \boldsymbol{\varphi} = \boldsymbol{\varphi}^* \right\} . \tag{1.96}$$

  Thus, all points in $\mathcal{Q}_{\rm s}(\boldsymbol{\varphi}^*)$ map onto the fixed point $\boldsymbol{\varphi}^*$ as $\tau \to \infty$, while all points in $\mathcal{Q}_{\rm u}(\boldsymbol{\varphi}^*)$ emanate from the fixed point $\boldsymbol{\varphi}^*$ as $\tau \to -\infty$.

- **Nodes** : When $0 < D < \frac{1}{4}T^2$, both eigenvalues are real and of the same sign. Thus, both right eigenvectors correspond to stable or to unstable directions, depending on whether $T < 0$ (stable; $\lambda_- < \lambda_+ < 0$) or $T < 0$ (unstable; $\lambda_+ > \lambda_- > 0$). If $\lambda_\pm$ are distinct, one can distinguish *fast* and *slow* eigendirections, based on the magnitude of the eigenvalues.

- **Spirals** : When $D > \frac{1}{4}T^2$, the discriminant $T^2 - 4D$ is negative, and the eigenvalues come in a complex conjugate pair: $\lambda_- = \lambda_+^*$. The real parts are given by $\mathrm{Re}(\lambda_\pm) = \frac{1}{2}T$, so the motion is stable (*i.e.* collapsing to the fixed point) if $T < 0$ and unstable (*i.e.* diverging from the fixed point) if $T > 0$.

  The motion is easily shown to correspond to a spiral. We write a general real linear

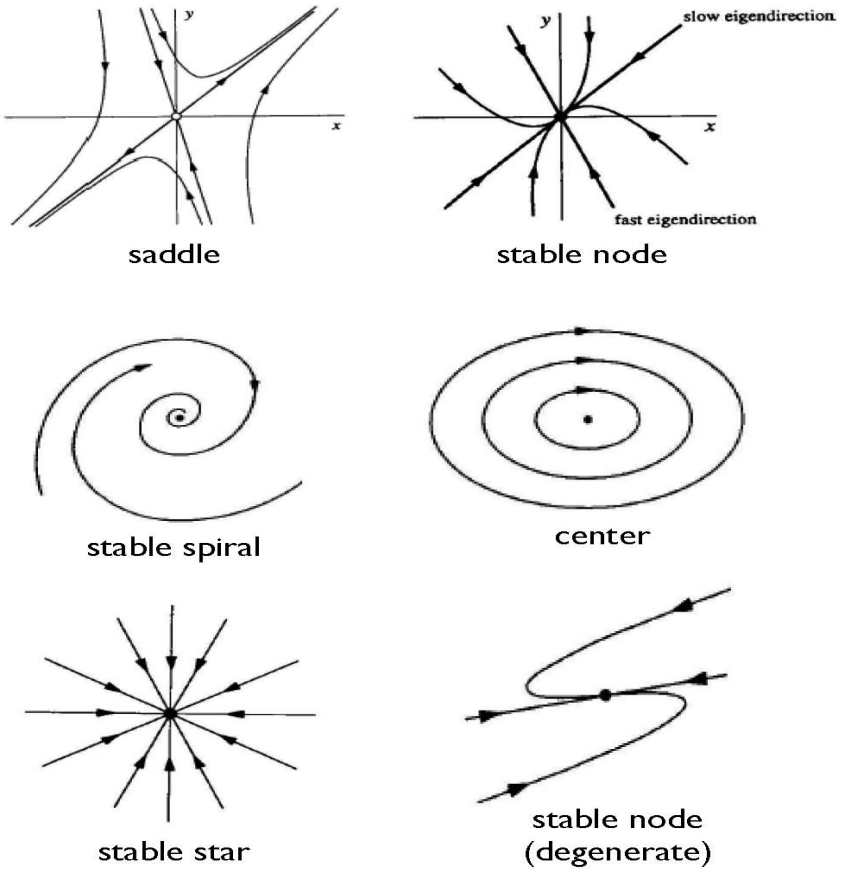

Figure 1.22: Fixed point zoo for $N = 2$ systems. Not shown: unstable versions of node, spiral, and star (reverse direction of arrows to turn stable into unstable).

combination of the two right eigenvectors,

$$\begin{pmatrix} u_1 \\ u_2 \end{pmatrix} = C_0\, e^{i\delta_0}\, e^{(\nu+i\omega)t} \begin{pmatrix} b \\ a-\nu-i\omega \end{pmatrix} + C_0\, e^{-i\delta_0}\, e^{(\nu-i\omega)t} \begin{pmatrix} b \\ a-\nu+i\omega \end{pmatrix}$$

$$= C_0\, e^{\nu t} \begin{pmatrix} b\,\cos(\omega t+\delta_0) \\ \sqrt{(a-\nu)^2+\omega^2}\,\cos\left(\omega t+\delta_0-\tan^{-1}\left(\frac{\omega}{a-\nu}\right)\right) \end{pmatrix} , \qquad (1.97)$$

with $\lambda_\pm = \nu \pm i\omega$, $\nu = \frac{1}{2}T = \frac{1}{2}(a+d)$, $\omega = \sqrt{T^2-4D} = \sqrt{(a-d)^2+4bc}$, and where C_0 and δ_0 are real constants. One can check that the spiral rotates counterclockwise for $a > d$ and clockwise for $a < d$.

- **Degenerate Cases** : When $T = 0$ we have $\lambda_\pm = \pm\sqrt{-D}$. For $D < 0$ we have a saddle, but for $D > 0$ both eigenvalues are imaginary: $\lambda_\pm = \pm i\sqrt{D}$. The orbits do

not collapse to a point, nor do they diverge to infinity, in the $t \to \infty$ limit, as they do in the case of the stable and unstable spiral. The fixed point is called a *center*, and it is surrounded by closed trajectories.

When $D = \frac{1}{4}T^2$, the discriminant vanishes and the eigenvalues are degenerate. If the rank of M is two, the fixed point is a stable ($T < 0$) or unstable ($T > 0$) *star*. If M is degenerate and of rank one, the fixed point is a *degenerate node*.

As an example, consider the matrix

$$M = \begin{pmatrix} a & b \\ 0 & c \end{pmatrix} \ . \tag{1.98}$$

If $b = 0$ and $c = a$, the fixed point is a star (stable if $a < 0$, and unstable if $a > 0$). If $b \neq 0$ and $c = a$, the star becomes a degenerate node. Let us maintain $c \neq a$ and exhibit all the eigenvectors of M. Clearly the eigenvalues are $\lambda_1 = a$ and $\lambda_2 = c$. One easily finds the normalized right and left eigenvectors:

$$\boldsymbol{\psi}_1 = \begin{pmatrix} 1 \\ 0 \end{pmatrix} \quad , \quad \boldsymbol{\chi}_1 = \begin{pmatrix} 1 & -\frac{b}{c-a} \end{pmatrix} \tag{1.99}$$

$$\boldsymbol{\psi}_2 = \begin{pmatrix} 1 \\ \frac{c-a}{b} \end{pmatrix} \quad , \quad \boldsymbol{\chi}_2 = \begin{pmatrix} 0 & \frac{b}{c-a} \end{pmatrix} \ . \tag{1.100}$$

As $c \to a$, ψ_2 approaches ψ_1, and the eigenspaces become parallel. Solving for the motion, one obtains

$$u_1(t) = \big(u_1(0) + b\, u_2(0)\, t\big)\, e^{at} \tag{1.101}$$

$$u_2(t) = u_2(0)\, e^{at} \ . \tag{1.102}$$

Note that the behavior is not purely exponential.

When $D = 0$, one of the eigenvalues vanishes. This indicates a *fixed line* in phase space, since any point on that line will not move. The fixed line can be stable or unstable, depending on whether the remaining eigenvalue is negative (stable, $T < 0$), or positive (unstable, $T > 0$).

Putting it all together, an example of a phase portrait is shown in Fig. 1.23. Note the presence of an *isolated, closed trajectory*, which is called a *limit cycle*.

1.6 Andronov-Hopf Bifurcation

A bifurcation between a spiral and a limit cycle is known as an *Andronov-Hopf bifurcation.* As a simple example, consider the $N = 2$ system,

$$\dot{x} = ax - by - C(x^2 + y^2)\, x \tag{1.103}$$

$$\dot{y} = bx + ay - C(x^2 + y^2)\, y \ , \tag{1.104}$$

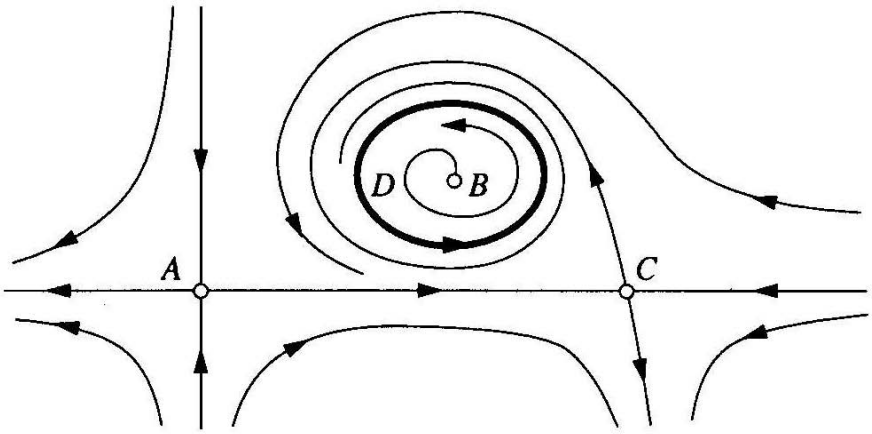

Figure 1.23: Phase portrait for an $N = 2$ flow including saddles (A,C), unstable spiral (B), and limit cycle (D).

where a, b, and C are real. Clearly the origin is a fixed point, at which one finds the eigenvalues $\lambda = a \pm ib$. Thus, the fixed point is a stable spiral if $a < 0$ and an unstable spiral if $a > 0$.

Written in terms of the complex variable $z = x + iy$, these two equations collapse to the single equation

$$\dot{z} = (a + ib)\, z - C\, |z|^2\, z \ . \tag{1.105}$$

The dynamics are also simple in polar coordinates $r = |z|$, $\theta = \arg(z)$:

$$\dot{r} = ar - Cr^3 \tag{1.106}$$

$$\dot{\theta} = b \ . \tag{1.107}$$

The phase diagram, for fixed $b > 0$, is depicted in Fig. 1.24. For positive a/C, there is a limit cycle at $r = \sqrt{a/C}$. In both cases, the limit cycle disappears as a crosses the value $a^* = 0$ and is replaced by a stable $(a < 0, C > 0)$ or unstable $(a > 0, C < 0)$ spiral.

This example also underscores the following interesting point. Adding a small nonlinear term C has no fundamental effect on the fixed point behavior so long as $a \neq 0$, when the fixed point is a stable or unstable spiral. In general, fixed points which are attractors (stable spirals or nodes), repellers (unstable spirals or nodes), or saddles are *robust* with respect to the addition of a small nonlinearity. But the fixed point behavior in the marginal cases – centers, stars, degenerate nodes, and fixed lines – is strongly affected by the presence of even a small nonlinearity. In this example, the FP is a center when $a = 0$. But as the (r, θ) dynamics shows, a small nonlinearity will destroy the center and turn the FP into an attractor $(C > 0)$ or a repeller $(C < 0)$.

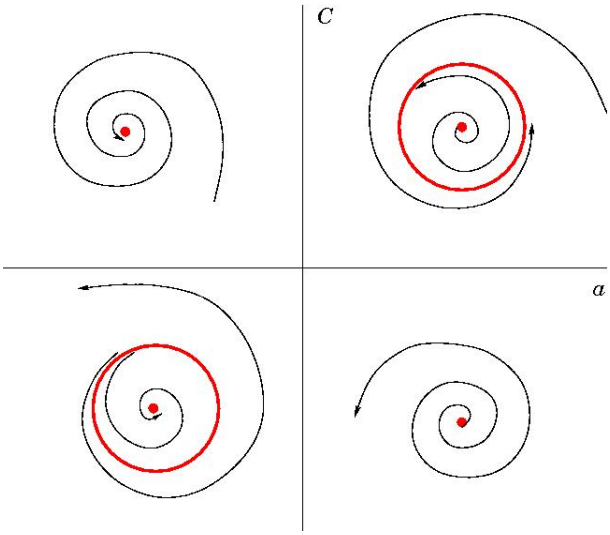

Figure 1.24: Hopf bifurcation: for $C > 0$ the bifurcation is supercritical, between stable spiral and stable limit cycle. For $C < 0$ the bifurcation is subcritical, between unstable spiral and unstable limit cycle. The bifurcation occurs at $a = 0$ in both cases.

1.6.1 Population Biology : Lotka-Volterra Models

Consider two species with populations N_1 and N_2, respectively. We model the evolution of these populations by the coupled ODEs

$$\frac{dN_1}{dt} = aN_1 + bN_1N_2 + cN_1^2 \tag{1.108}$$

$$\frac{dN_2}{dt} = dN_2 + eN_1N_2 + fN_2^2 \ , \tag{1.109}$$

where $\{a, b, c, d, e, f\}$ are constants. We can eliminate some constants by rescaling. Let us define

$$N_1 \equiv \mu x \quad , \quad N_2 \equiv \nu y \quad , \quad t \equiv \kappa s \ . \tag{1.110}$$

Thus, x is the rescaled population N_1 and y is the rescaled population N_2; the dimensionless time variable is s. We now have

$$\frac{dx}{ds} = \kappa a\, x + \kappa\nu b\, xy + \kappa\mu c\, x^2 \tag{1.111}$$

$$\frac{dy}{ds} = \kappa d\, y + \kappa\mu e\, xy + \kappa\nu f\, y^2 \ . \tag{1.112}$$

Since the independent variables here represent populations, we would like all the rescaling factors to be positive. We may now demand

$$\kappa|a| = 1 \ , \ \kappa|b|\nu = 1 \ , \ \kappa|e|\mu = 1 \quad \Longrightarrow \quad \kappa = \frac{1}{|a|} \ , \ \mu = \frac{|a|}{|e|} \ , \ \nu = \frac{|a|}{|b|} \tag{1.113}$$

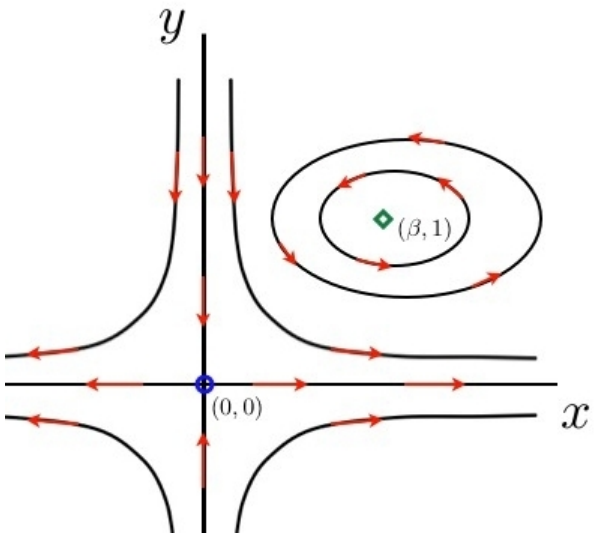

Figure 1.25: Phase flow for the rabbits *vs.* foxes Lotka-Volterra model of eq. 1.117.

This results in the following:

$$\dot{x} = \sigma x + \sigma' xy + Ax^2 \tag{1.114}$$

$$\dot{y} = By + \sigma'' xy + Cy^2 \ , \tag{1.115}$$

where $\sigma = \text{sgn}\,(a)$, $\sigma' = \text{sgn}\,(b)$, and $\sigma'' = \text{sgn}\,(e)$ can each take on one of two possible values ± 1. The remaining coefficients may be of either sign, and are related to the original ones as

$$A = \frac{c}{|e|} \quad , \quad B = \frac{d}{|a|} \quad , \quad C = \frac{f}{|b|} \ . \tag{1.116}$$

The values and especially the signs of the various coefficients have a physical (or biological) significance. For example, if $\sigma' > 0$ it means that x grows due to the presence of y. The effect of y on x may be of the same sign ($\sigma'\sigma'' = 1$) or of opposite sign ($\sigma'\sigma'' = -1$).

As an example, consider the model

$$\dot{x} = x - xy \quad , \quad \dot{y} = -\beta y + xy \ . \tag{1.117}$$

The quantity x might represent the (scaled) population of rabbits and y the population of foxes in an ecosystem. There are two fixed points – at $(0, 0)$ and at $(\beta, 1)$. Linearizing the dynamics about these fixed points, one finds that $(0, 0)$ is a saddle while $(\beta, 1)$ is a center. Let's do this explicitly.

The first step is to find the fixed points (x^*, y^*). To do this, we set $\dot{x} = 0$ and $\dot{y} = 0$. From $\dot{x} = x(1 - y) = 0$ we have that $x = 0$ or $y = 1$. Suppose $x = 0$. The second equation, $\dot{y} = (x - \beta)y$ then requires $y = 0$. So $\text{P}_1 = (0, 0)$ is a fixed point. The other possibility is that $y = 1$, which then requires $x = \beta$. So $\text{P}_2 = (\beta, 1)$ is the second fixed point. Those are the only possibilities.

We now compute the linearized dynamics at these fixed points. The linearized dynamics are given by $\dot{\boldsymbol{\varphi}} = M\boldsymbol{\varphi}$, with

$$M = \begin{pmatrix} \partial\dot{x}/\partial x & \partial\dot{x}/\partial y \\ \partial\dot{y}/\partial x & \partial\dot{y}/\partial y \end{pmatrix} = \begin{pmatrix} 1-y & -x \\ y & x-\beta \end{pmatrix} \ . \tag{1.118}$$

Evaluating M at P_1 and P_2, we find

$$M_1 = \begin{pmatrix} 1 & 0 \\ 0 & -\beta \end{pmatrix} \quad , \quad M_2 = \begin{pmatrix} 0 & -\beta \\ 1 & 0 \end{pmatrix} \ . \tag{1.119}$$

The eigenvalues are easily found:

$$\mathrm{P}_1 \ : \ \lambda_+ = 1 \qquad\qquad \mathrm{P}_2 \ : \ \lambda_+ = i\sqrt{\beta} \tag{1.120}$$

$$\lambda_- = -\beta \qquad\qquad \lambda_- = -i\sqrt{\beta} \ . \tag{1.121}$$

Thus P_1 is a saddle point and P_2 is a center.

In the rabbits and foxes model of eq. 1.117, the rabbits are the food for the foxes. This means $\sigma' = -1$ but $\sigma'' = +1$ – the fox population is enhanced by the presence of rabbits, but the rabbit population is diminished by the presence of foxes. Consider now a model in which the two species (rabbits and sheep, say) compete for food:

$$\dot{x} = x - xy - Ax^2 \quad , \quad \dot{y} = By - xy - Cy^2 \ , \tag{1.122}$$

with A, B, and C all positive. Note that when either population x or y vanishes, the remaining population is governed by the logistic equation, *i.e.* it will flow to a nonzero fixed point.

The matrix of derivatives, which is to be evaluated at each fixed point in order to assess its stability, is

$$M = \begin{pmatrix} \partial\dot{x}/\partial x & \partial\dot{x}/\partial y \\ \partial\dot{y}/\partial x & \partial\dot{y}/\partial y \end{pmatrix} = \begin{pmatrix} 1-y-2Ax & -x \\ -y & B-x-2Cy \end{pmatrix} \ . \tag{1.123}$$

At each fixed point, we must evaluate $D = \det(M)$ and $T = \mathrm{Tr}\,(M)$ and apply the classification scheme of Fig. 1.21.

1. $\mathrm{P}_1 = (0,0)$. This is the trivial state with no rabbits ($x = 0$) and no sheep ($y = 0$). The linearized dynamics gives $M_1 = \begin{pmatrix} 1 & 0 \\ 0 & B \end{pmatrix}$, which corresponds to an unstable node.

2. $\mathrm{P}_2 = (A^{-1}, 0)$. Here we have rabbits but no sheep. The linearized dynamics gives $M_2 = \begin{pmatrix} 1 & -A^{-1} \\ 0 & B - A^{-1} \end{pmatrix}$. For $AB > 1$ this is a saddle; for $AB < 1$ it is a stable node.

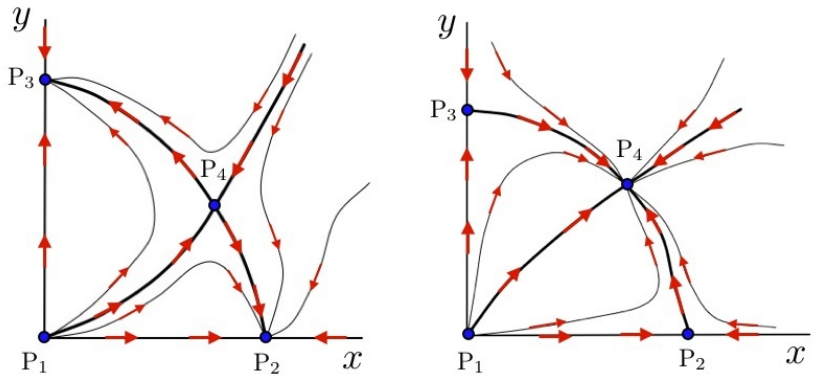

Figure 1.26: Two possible phase flows for the rabbits *vs.* sheep model of eq. 1.122.

3. $\mathrm{P}_3 = (0, C^{-1}B)$. Here we have sheep but no rabbits. The linearized dynamics gives $M_3 = \begin{pmatrix} 1 - C^{-1}B & 0 \\ -C^{-1}B & -B \end{pmatrix}$. For $B > C$ this is a stable node; for $B < C$ it is a saddle.

4. There is one remaining fixed point – a nontrivial one where both x and y are nonzero. To find it, we set $\dot{x} = \dot{y} = 0$, and divide out by x and y respectively, to get

$$Ax + y = 1 \quad , \quad x + Cy = B \ , \tag{1.124}$$

the solution of which is

$$\mathrm{P}_4 = \left(\frac{B - C}{1 - AC} \ , \ \frac{1 - AB}{1 - AC} \right) . \tag{1.125}$$

The linearized dynamics then gives

$$M_4 = \frac{1}{1 - AC} \begin{pmatrix} AC - AB & C - B \\ AB - 1 & ABC - C \end{pmatrix} \ , \tag{1.126}$$

giving

$$T = \frac{AC + ABC - AB - C}{1 - AC} \quad , \quad D = \frac{(B - C)(AB - 1)}{1 - AC} \ . \tag{1.127}$$

The classification of this fixed point can vary with parameters. For example, if $A = 1$, $B = \frac{1}{2}$, and $C = \frac{1}{4}$, find $T = -\frac{1}{2}$ and $D = -\frac{1}{6}$, corresponding to a saddle point. In this case, it is the fate of one population to die out at the expense of the other. Note that $AB < 1$ and $B > C$, so P_2 and P_3 are both stable nodes. Which species lives and which dies depends on initial conditions. If on the other hand $A = 2$, $B = 1$, and $C = 2$, find $T = -\frac{4}{3}$ and $D = \frac{1}{3}$, and P_4 is a stable node, while P_2 and P_3 are saddles. The situation is depicted in Fig. 1.26.

1.7 Linear Oscillations

We begin with the homogeneous equation for a damped harmonic oscillator,

$$\frac{d^2x}{dt^2} + 2\beta\,\frac{dx}{dt} + \omega_0^2\,x = 0\ . \tag{1.128}$$

To solve, write $x(t) = \sum_i C_i\,e^{-i\omega_i t}$. This renders the differential equation 1.128 an *algebraic* equation for the two eigenfrequencies ω_i, each of which must satisfy

$$\omega^2 + 2i\beta\omega - \omega_0^2 = 0\ , \tag{1.129}$$

hence

$$\omega_\pm = -i\beta \pm (\omega_0^2 - \beta^2)^{1/2} \tag{1.130}$$

and the most general solution to 1.128 is

$$x(t) = C_+\,e^{-i\omega_+ t} + C_-\,e^{-i\omega_- t} \tag{1.131}$$

where $C_\pm$ are arbitrary constants. Notice that the eigenfrequencies are in general complex, with a negative imaginary part (so long as the damping coefficient β is positive). Thus $e^{-i\omega_\pm t}$ decays to zero as $t \to \infty$.

Classification of Damped Harmonic Motion

We identify three classes of motion:

$$\begin{aligned}
\text{(i) Underdamped } (\omega_0^2 > \beta^2): \quad x(t) &= C\,e^{-\beta t}\cos(\nu t) + D\,e^{-\beta t}\sin(\nu t) \\
\text{(ii) Overdamped } (\omega_0^2 < \beta^2): \quad x(t) &= C\,e^{-\beta t}\cosh(\nu t) + C\,e^{-\beta t}\sinh(\nu t) \\
\text{(iii) Critically Damped } (\omega_0^2 = \beta^2): \quad x(t) &= C\,e^{-\beta t} + D\,t\,e^{-\beta t}
\end{aligned}$$

where $\nu \equiv |\omega_0^2 - \beta^2|^{1/2}$.

1.7.1 Solution to the Inhomogeneous Equation

When forced, the equation for the damped oscillator becomes

$$\frac{d^2x}{dt^2} + 2\beta\,\frac{dx}{dt} + \omega_0^2\,x = f(t)\ . \tag{1.132}$$

Since this equation is linear in $x(t)$, we can, without loss of generality, restrict out attention to harmonic forcing terms of the form

$$f(t) = f_0\cos(\Omega t + \varphi_0) = \mathrm{Re}\Big[f_0\,e^{-i\varphi_0}\,e^{-i\Omega t}\Big] \tag{1.133}$$

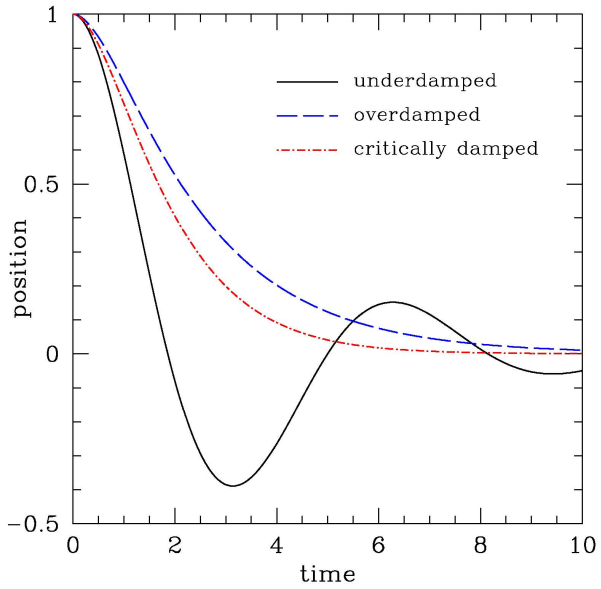

Figure 1.27: Three classifications of damped harmonic motion.

where Re stands for "real part". Here, Ω is the forcing frequency. We try a solution $x(t) = x_0\, e^{-i\Omega t}$. Substituting this form into equation 1.132, we find a solution

$$x_{\rm i}(t) = {\rm Re}[A(\Omega)\, e^{i\delta(\Omega)} \cdot f_0\, e^{-i\varphi_0}\, e^{-i\Omega t}] \tag{1.134}$$

$$A(\Omega) = \Big((\omega_0^2 - \Omega^2)^2 + 4\beta^2\Omega^2\Big)^{-1/2} \tag{1.135}$$

$$\delta(\Omega) = \tan^{-1}\left(\frac{2\beta\Omega}{\omega_0^2 - \Omega^2}\right)\ . \tag{1.136}$$

The quantity $A(\Omega)$ is the *amplitude* of the response (in units of f_0), while $\delta(\Omega)$ is the (dimensionless) *phase lag*.

Since equation 1.132 is linear, we can add a solution to the homogeneous equation to $x_{\rm i}(t)$ and we still have a solution. Thus, the most general solution to eqn. 1.132 is

$$x(t) = {\rm Re}\Big[A(\Omega)\, e^{i\delta(\Omega)} \cdot f_0\, e^{-i\varphi_0}\, e^{-i\Omega t}\Big] + C_+\, e^{-i\omega_+ t} + C_-\, e^{-i\omega_- t}\ . \tag{1.137}$$

1.7.2 General Solution by Green's Function Method

For a general forcing function $f(t)$, we solve by Fourier transform. Recall that a function $F(t)$ in the time domain has a Fourier transform $\hat{F}(\omega)$ in the frequency domain. The relation

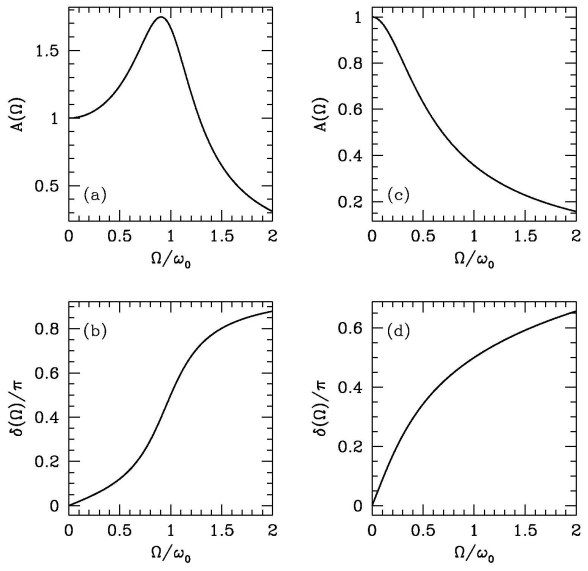

Figure 1.28: Amplitude and phase shift *versus* oscillator frequency (units of ω_0) for underdamped oscillator (a,b) with $\beta = 0.3\,\omega_0$ and for overdamped oscillator (c,d) with $\beta = 1.4\,\omega_0$.

between the two is:

$$F(t) = \int_{-\infty}^{\infty} \frac{d\omega}{2\pi}\, e^{-i\omega t}\, \hat{F}(\omega) \quad \Longleftrightarrow \quad \hat{F}(\omega) = \int_{-\infty}^{\infty} dt\, e^{+i\omega t}\, F(t)\ . \tag{1.138}$$

We can convert the differential equation 1.28 to an algebraic equation in the frequency domain, $\hat{x}(\omega) = \hat{G}(\omega)\,\hat{f}(\omega)$, where

$$\hat{G}(\omega) = \frac{1}{\omega_0^2 - 2i\beta\omega - \omega^2} \tag{1.139}$$

is the *Green's function* in the frequency domain. The general solution is written

$$x(t) = \int_{-\infty}^{\infty} \frac{d\omega}{2\pi}\, e^{-i\omega t}\, \hat{G}(\omega)\, \hat{f}(\omega) + x_{\rm h}(t)\ , \tag{1.140}$$

where $x_{\rm h}(t) = \sum_i C_i\, e^{-i\omega_i t}$ is a solution to the homogeneous equation. We may also write the above integral over the time domain:

$$x(t) = \int_{-\infty}^{\infty} dt'\, G(t-t')\, f(t') + x_{\rm h}(t) \tag{1.141}$$

$$\begin{aligned} G(s) &= \int_{-\infty}^{\infty} \frac{d\omega}{2\pi}\, e^{-i\omega s}\, \hat{G}(\omega) \\ &= \nu^{-1}\, \exp(-\beta s)\, \sin(\nu s)\, \Theta(s) \end{aligned} \tag{1.142}$$

where $\Theta(s)$ is the *step function*,

$$\Theta(s) = \begin{cases} 1 & \text{if } s \geq 0 \\ 0 & \text{if } s < 0 \end{cases} \tag{1.143}$$

Example: Pulse Force

Consider a pulse force

$$f(t) = f_0\,\Theta(t)\,\Theta(T-t) = \begin{cases} f_0 & \text{if } 0 \leq t \leq T \\ 0 & \text{otherwise.} \end{cases} \tag{1.144}$$

In the underdamped regime, for example, we find the solution

$$x(t) = \frac{f_0}{\omega_0^2}\left\{1 - e^{-\beta t}\cos\nu t - \frac{\beta}{\nu}e^{-\beta t}\sin\nu t\right\} \tag{1.145}$$

if $0 \leq t \leq T$ and

$$\begin{aligned} x(t) \;\; = \;\; & \frac{f_0}{\omega_0^2}\left\{\left(e^{-\beta(t-T)}\cos\nu(t-T) - e^{-\beta t}\cos\nu t\right)\right. \\ & \left. + \frac{\beta}{\nu}\left(e^{-\beta(t-T)}\sin\nu(t-T) - e^{-\beta t}\sin\nu t\right)\right\} \end{aligned} \tag{1.146}$$

if $t > T$.

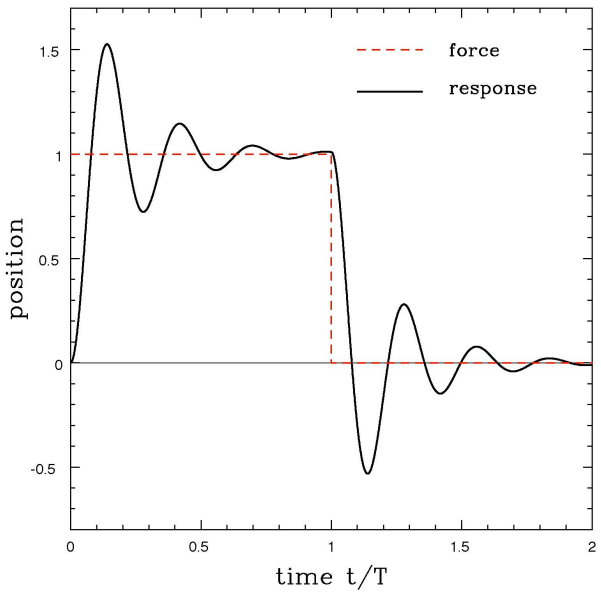

Figure 1.29: Response of an underdamped oscillator to a pulse force.

1.8 General Linear Autonomous Inhomogeneous ODEs

This method immediately generalizes to the case of general autonomous linear inhomogeneous ODEs of the form

$$\frac{d^n x}{dt^n} + a_{n-1}\,\frac{d^{n-1}x}{dt^{n-1}} + \ldots + a_1\,\frac{dx}{dt} + a_0\,x = f(t)\ . \tag{1.147}$$

We can write this as

$$L_t\,x(t) = f(t)\ , \tag{1.148}$$

where L_t is the $n^{\rm th}$ order differential operator

$$L_t = \frac{d^n}{dt^n} + a_{n-1}\,\frac{d^{n-1}}{dt^{n-1}} + \ldots + a_1\,\frac{d}{dt} + a_0\ . \tag{1.149}$$

The general solution to the inhomogeneous equation is given by

$$x(t) = x_{\rm h}(t) + \int_{-\infty}^{\infty} dt'\,G(t,t')\,f(t')\ , \tag{1.150}$$

where $G(t,t')$ is the Green's function. Note that $L_t\,x_{\rm h}(t) = 0$. Thus, we must have

$$L_t\,G(t,t') = \delta(t-t')\ . \tag{1.151}$$

If the differential equation $L_t\,x(t) = f(t)$ is defined over some finite t interval with prescribed boundary conditions on $x(t)$ at the endpoints, then $G(t,t')$ will depend on t and t' separately. For the case we are considering, the interval is the entire real line $t \in (-\infty,\infty)$, and $G(t,t') = G(t-t')$ is a function of the single variable $t-t'$.

Note that $L_t = L\big(\frac{d}{dt}\big)$ may be regarded as a function of the differential operator $\frac{d}{dt}$. If we now Fourier transform the equation $L_t\,x(t) = f(t)$, we obtain

$$\hat{L}(\omega)\,\hat{x}(\omega) = \hat{f}(\omega)\ , \tag{1.152}$$

with

$$\hat{L}(\omega) = \sum_{k=0}^{n} a_k\,(-i\omega)^k\ , \tag{1.153}$$

where $a_n \equiv 1$. According to the Fundamental Theorem of Algebra, the $n^{\rm th}$ degree polynomial $\hat{L}(\omega)$ may be uniquely factored over the complex ω plane into a product over n roots:

$$\hat{L}(\omega) = (-i)^n\,(\omega-\omega_1)(\omega-\omega_2)\cdots(\omega-\omega_n)\ . \tag{1.154}$$

If the $\{a_k\}$ are all real, then $\big[\hat{L}(\omega)\big]^* = \hat{L}(-\omega^*)$, hence if Ω is a root then so is $-\Omega^*$. Thus, the roots appear in pairs which are symmetric about the imaginary axis. *I.e.* if $\Omega = a + ib$ is a root, then so is $-\Omega^* = -a + ib$.

The general solution to the homogeneous equation is

$$x_{\rm h}(t) = \sum_{i=1}^{n} A_i \, e^{-i\omega_i t} \ , \tag{1.155}$$

which involves n arbitrary complex constants A_i. The susceptibility, or Green's function in Fourier space, $\hat{G}(\omega)$ is then

$$\hat{G}(\omega) = \frac{1}{\hat{L}(\omega)} = \frac{i^n}{(\omega-\omega_1)(\omega-\omega_2)\cdots(\omega-\omega_n)} \ , \tag{1.156}$$

and the general solution to the inhomogeneous equation is again given by

$$x(t) = x_{\rm h}(t) + \int_{-\infty}^{\infty} dt' \, G(t-t') \, f(t') \ , \tag{1.157}$$

where $x_{\rm h}(t)$ is the solution to the homogeneous equation, *i.e.* with zero forcing, and where

$$\begin{aligned} G(s) &= \int\limits_{-\infty}^{\infty} \frac{d\omega}{2\pi} \, e^{-i\omega s} \, \hat{G}(\omega) \\ &= i^n \int_{-\infty}^{\infty} \frac{d\omega}{2\pi} \, \frac{e^{-i\omega s}}{(\omega-\omega_1)(\omega-\omega_2)\cdots(\omega-\omega_n)} \\ &= \sum_{j=1}^{n} \frac{e^{-i\omega_j s}}{iL'(\omega_j)} \, \Theta(s) \ , \end{aligned} \tag{1.158}$$

where we assume that $\mathrm{Im}\,(\omega_j) < 0$ for all j, which is necessary in order that the response be causal. One can check that for the familiar case $L_t = d_t^2 + 2\beta d_t + \omega_0^2$ that $G(s) = \nu^{-1} \, e^{-\beta s} \, \sin(\nu s) \, \Theta(s)$.

1.8.1 Kramers-Krönig Relations

Suppose $\hat{\chi}(\omega) \equiv \hat{G}(\omega)$ is analytic in the UHP[5]. Then for all ν, we must have

$$\int_{-\infty}^{\infty} \frac{d\nu}{2\pi} \, \frac{\hat{\chi}(\nu)}{\nu - \omega + i\epsilon} = 0 \ , \tag{1.159}$$

where ϵ is a positive infinitesimal. The reason is simple: just close the contour in the UHP, assuming $\hat{\chi}(\omega)$ vanishes sufficiently rapidly that Jordan's lemma can be applied. Clearly this is an extremely weak restriction on $\hat{\chi}(\omega)$, given the fact that the denominator already causes the integrand to vanish as $|\omega|^{-1}$.

Let us examine the function

$$\frac{1}{\nu - \omega + i\epsilon} = \frac{\nu-\omega}{(\nu-\omega)^2 + \epsilon^2} - \frac{i\epsilon}{(\nu-\omega)^2 + \epsilon^2} \ . \tag{1.160}$$

[5]In this section, we use the notation $\hat{\chi}(\omega)$ for the susceptibility, rather than $\hat{G}(\omega)$

which we have separated into real and imaginary parts. Under an integral sign, the first term, in the limit $\epsilon \to 0$, is equivalent to taking a *principal part* of the integral. That is, for any function $F(\nu)$ which is regular at $\nu = \omega$,

$$\lim_{\epsilon\to 0} \int_{-\infty}^{\infty} \frac{d\nu}{2\pi} \, \frac{\nu - \omega}{(\nu-\omega)^2 + \epsilon^2} \, F(\nu) \equiv \mathcal{P} \int_{-\infty}^{\infty} \frac{d\nu}{2\pi} \, \frac{F(\nu)}{\nu - \omega} \ . \tag{1.161}$$

The principal part symbol $\mathcal{P}$ means that the singularity at $\nu = \omega$ is elided, either by smoothing out the function $1/(\nu-\epsilon)$ as above, or by simply cutting out a region of integration of width ϵ on either side of $\nu = \omega$.

The imaginary part is more interesting. Let us write

$$h(u) \equiv \frac{\epsilon}{u^2 + \epsilon^2} \ . \tag{1.162}$$

For $|u| \gg \epsilon$, $h(u) \simeq \epsilon/u^2$, which vanishes as $\epsilon \to 0$. For $u = 0$, $h(0) = 1/\epsilon$ which diverges as $\epsilon \to 0$. Thus, $h(u)$ has a huge peak at $u = 0$ and rapidly decays to 0 as one moves off the peak in either direction a distance greater that ϵ. Finally, note that

$$\int_{-\infty}^{\infty} du \, h(u) = \pi \ , \tag{1.163}$$

a result which itself is easy to show using contour integration. Putting it all together, this tells us that

$$\lim_{\epsilon\to 0} \frac{\epsilon}{u^2 + \epsilon^2} = \pi\delta(u) \ . \tag{1.164}$$

Thus, for positive infinitesimal ϵ,

$$\frac{1}{u \pm i\epsilon} = \mathcal{P}\,\frac{1}{u} \mp i\pi\delta(u) \ , \tag{1.165}$$

a most useful result.

We now return to our initial result 1.159, and we separate $\hat{\chi}(\omega)$ into real and imaginary parts:

$$\hat{\chi}(\omega) = \hat{\chi}'(\omega) + i\hat{\chi}''(\omega) \ . \tag{1.166}$$

We therefore have, for every real value of ω,

$$0 = \int_{-\infty}^{\infty} \frac{d\nu}{2\pi} \Big[\chi'(\nu) + i\chi''(\nu)\Big] \Big[\mathcal{P}\,\frac{1}{\nu-\omega} - i\pi\delta(\nu-\omega)\Big] \ . \tag{1.167}$$

Taking the real and imaginary parts of this equation, we derive the *Kramers-Krönig relations*:

$$\chi'(\omega) \;=\; +\mathcal{P}\!\int_{-\infty}^{\infty} \frac{d\nu}{\pi} \, \frac{\hat{\chi}''(\nu)}{\nu-\omega} \tag{1.168}$$

$$\chi''(\omega) \;=\; -\mathcal{P}\!\int_{-\infty}^{\infty} \frac{d\nu}{\pi} \, \frac{\hat{\chi}'(\nu)}{\nu-\omega} \ . \tag{1.169}$$

1.8.2 Resonant Forcing

When the damping β vanishes, the response diverges at resonance. The solution to the resonantly forced oscillator

$$\ddot{x} + \Omega_0^2\, x = \, f_0 \cos(\Omega_0 t + \varphi) \tag{1.170}$$

is

$$x(t) = \frac{f_0}{2\Omega_0}\, t\, \sin(\Omega_0 t + \varphi) + x_{\rm h}(t)\ . \tag{1.171}$$

The amplitude of this solution grows linearly due to the energy pumped into the oscillator by the resonant external forcing. As we shall now learn, nonlinearities can mitigate this unphysical, unbounded response.

1.9 Nonlinear Oscillators

Consider a nonlinear oscillator described by the equation of motion

$$\ddot{x} + \Omega_0^2\, x = \epsilon\, h(x)\ . \tag{1.172}$$

Here, ϵ is a dimensionless parameter, assumed to be small, and $h(x)$ is a nonlinear function of x. In general, we might consider equations of the form

$$\ddot{x} + \Omega_0^2\, x = \epsilon\, h(x, \dot{x})\ , \tag{1.173}$$

such as the van der Pol oscillator,

$$\ddot{x} + \mu(x^2 - 1)\dot{x} + \Omega_0^2\, x = 0\ . \tag{1.174}$$

First, we will focus on nondissipative systems, *i.e.* where we may write $m\ddot{x} = -\partial_x V$, with $V(x)$ some potential.

As an example, consider the simple pendulum, which obeys

$$\ddot{\theta} + \Omega_0^2 \sin\theta = 0\ , \tag{1.175}$$

where $\Omega_0^2 = g/\ell$, with ℓ the length of the pendulum. We may rewrite his equation as

$$\begin{aligned} \ddot{\theta} + \Omega_0^2\, \theta &= \Omega_0^2\, (\theta - \sin\theta) \\ &= \tfrac{1}{6}\, \Omega_0^2\, \theta^3 - \tfrac{1}{120}\, \Omega_0^2\, \theta^5 + \ldots \end{aligned} \tag{1.176}$$

The RHS above is a nonlinear function of θ. We can define this to be $h(\theta)$, and take $\epsilon = 1$.

1.9.1 Naïve Perturbation Theory and its Failure

Let's assume though that ϵ is small, and write a formal power series expansion of the solution $x(t)$ to equation 1.172 as

$$x = x_0 + \epsilon\, x_1 + \epsilon^2\, x_2 + \dots \ . \tag{1.177}$$

We now plug this into 1.172. We need to use Taylor's theorem,

$$h(x_0 + \eta) = h(x_0) + h'(x_0)\,\eta + \tfrac{1}{2}\,h''(x_0)\,\eta^2 + \dots \tag{1.178}$$

with

$$\eta = \epsilon\, x_1 + \epsilon^2\, x_2 + \dots \ . \tag{1.179}$$

Working out the resulting expansion in powers of ϵ is tedious. One finds

$$h(x) = h(x_0) + \epsilon\, h'(x_0)\, x_1 + \epsilon^2 \left\{ h'(x_0)\, x_2 + \tfrac{1}{2}\, h''(x_0)\, x_1^2 \right\} + \dots \ . \tag{1.180}$$

Equating terms of the same order in ϵ, we obtain a hierarchical set of equations,

$$\ddot{x}_0 + \Omega_0^2\, x_0 = 0 \tag{1.181}$$

$$\ddot{x}_1 + \Omega_0^2\, x_1 = h(x_0) \tag{1.182}$$

$$\ddot{x}_2 + \Omega_0^2\, x_2 = h'(x_0)\, x_1 \tag{1.183}$$

$$\ddot{x}_3 + \Omega_0^2\, x_3 = h'(x_0)\, x_2 + \tfrac{1}{2}\, h''(x_0)\, x_1^2 \tag{1.184}$$

et cetera, where prime denotes differentiation with respect to argument. The first of these is easily solved: $x_0(t) = A\,\cos(\Omega_0 t + \varphi)$, where A and φ are constants. This solution then is plugged in at the next order, to obtain an inhomogeneous equation for $x_1(t)$. Solve for $x_1(t)$ and insert into the following equation for $x_2(t)$, *etc.* It looks straightforward enough.

The problem is that resonant forcing terms generally appear in the RHS of each equation of the hierarchy past the first. Define $\theta \equiv \Omega_0 t + \varphi$. Then $x_0(\theta)$ is an even periodic function of θ with period 2π, hence so is $h(x_0)$. We may then expand $h\big(x_0(\theta)\big)$ in a Fourier series:

$$h\big(A\cos\theta\big) = \sum_{n=0}^{\infty} h_n(A)\ \cos(n\theta)\ . \tag{1.185}$$

The $n = 1$ term leads to resonant forcing. Thus, the solution for $x_1(t)$ is

$$x_1(t) = \sum_{\substack{n=0 \\ (n\neq 1)}}^{\infty} \frac{h_n(A)}{1-n^2}\ \cos(n\Omega_0 t + n\varphi) + \frac{h_1(A)}{2\Omega_0}\, t\ \sin(\Omega_0 t + \varphi)\ , \tag{1.186}$$

which increases linearly with time. As an example, consider a cubic nonlinearity with $h(x) = r\,x^3$, where r is a constant. Then using

$$\cos(3\theta) = \tfrac{3}{4}\cos(\theta) + \tfrac{1}{4}\cos(3\theta)\ , \tag{1.187}$$

we have $h_1 = \frac{3}{4}\,rA^3$, $h_3 = \frac{1}{4}\,rA^3$.

1.9.2 Poincaré-Lindstedt Method

The problem here is that the nonlinear oscillator has a different frequency than its linear counterpart. Indeed, if we assume the frequency Ω is a function of ϵ, with

$$\Omega(\epsilon) = \Omega_0 + \epsilon\,\Omega_1 + \epsilon^2\Omega_2 + \ldots \ , \tag{1.188}$$

then subtracting the unperturbed solution from the perturbed one and expanding in ϵ yields

$$\begin{aligned}\cos(\Omega t) - \cos(\Omega_0 t) &= -\sin(\Omega_0 t)\,(\Omega - \Omega_0)\,t - \tfrac{1}{2}\cos(\Omega_0 t)\,(\Omega - \Omega_0)^2\,t^2 + \ldots \\ &= -\epsilon\,\sin(\Omega_0 t)\,\Omega_1 t - \epsilon^2\Big\{\sin(\Omega_0 t)\,\Omega_2 t + \tfrac{1}{2}\cos(\Omega_0 t)\,\Omega_1^2 t^2\Big\} + \mathcal{O}(\epsilon^3)\ .\end{aligned} \tag{1.189}$$

What perturbation theory can do for us is to provide a good solution *up to a given time*, provided that ϵ is *sufficiently small*. It *will not* give us a solution that is close to the true answer for *all* time. We see above that in order to do that, and to recover the shifted frequency $\Omega(\epsilon)$, we would have to resum perturbation theory to all orders, which is a daunting task.

The Poincaré-Lindstedt method obviates this difficulty by assuming $\Omega = \Omega(\epsilon)$ from the outset. Define a dimensionless time $s \equiv \Omega t$ and write 1.172 as

$$\Omega^2\,\frac{d^2x}{ds^2} + \Omega_0^2\,x = \epsilon\,h(x)\ , \tag{1.190}$$

where

$$x = x_0 + \epsilon\,x_1 + \epsilon^2\,x_2 + \ldots \tag{1.191}$$

$$\Omega^2 = a_0 + \epsilon\,a_1 + \epsilon^2\,a_2 + \ldots\ . \tag{1.192}$$

We now plug the above expansions into 1.190:

$$\begin{aligned}&\big(a_0 + \epsilon\,a_1 + \epsilon^2\,a_2 + \ldots\big)\left(\frac{d^2x_0}{ds^2} + \epsilon\,\frac{d^2x_1}{ds^2} + \epsilon^2\,\frac{d^2x_2}{ds^2} + \ldots\right) \\ &\qquad + \Omega_0^2\,\big(x_0 + \epsilon\,x_1 + \epsilon^2\,x_2 + \ldots\big) \\ &= \epsilon\,h(x_0) + \epsilon^2\,h'(x_0)\,x_1 + \epsilon^3\left\{h'(x_0)\,x_2 + \tfrac{1}{2}\,h''(x_0)\,x_1^2\right\} + \ldots\end{aligned} \tag{1.193}$$

Now let's write down equalities at each order in ϵ:

$$a_0\,\frac{d^2x_0}{ds^2} + \Omega_0^2\,x_0 = 0 \tag{1.194}$$

$$a_0\,\frac{d^2x_1}{ds^2} + \Omega_0^2\,x_1 = h(x_0) - a_1\,\frac{d^2x_0}{ds^2} \tag{1.195}$$

$$a_0\,\frac{d^2x_2}{ds^2} + \Omega_0^2\,x_2 = h'(x_0)\,x_1 - a_2\,\frac{d^2x_0}{ds^2} - a_1\,\frac{d^2x_1}{ds^2}\ , \tag{1.196}$$

et cetera.

The first equation of the hierarchy is immediately solved by

$$a_0 = \Omega_0^2 \qquad , \qquad x_0(s) = A\,\cos(s+\varphi)\ . \tag{1.197}$$

At $\mathcal{O}(\epsilon)$, then, we have

$$\frac{d^2x_1}{ds^2} + x_1 = \Omega_0^{-2}\,h\big(A\cos(s+\varphi)\big) + \Omega_0^{-2}\,a_1\,A\cos(s+\varphi)\ . \tag{1.198}$$

The LHS of the above equation has a natural frequency of unity (in terms of the dimensionless time s). We expect $h(x_0)$ to contain resonant forcing terms, per 1.185. However, we now have the freedom to adjust the undetermined coefficient a_1 to *cancel* any such resonant term. Clearly we must choose

$$a_a = -\frac{h_1(A)}{A}\ . \tag{1.199}$$

The solution for $x_1(s)$ is then

$$x_1(s) = \frac{1}{\Omega_0^2}\sum_{\substack{n=0\\(n\neq 1)}}^{\infty}\frac{h_n(A)}{1-n^2}\,\cos(ns+n\varphi)\ , \tag{1.200}$$

which is periodic and hence does not increase in magnitude without bound, as does 1.186. The perturbed frequency is then obtained from

$$\Omega^2 = \Omega_0^2 - \frac{h_1(A)}{A}\,\epsilon + \mathcal{O}(\epsilon^2) \quad\Longrightarrow\quad \Omega(\epsilon) = \Omega_0 - \frac{h_1(A)}{2A\Omega_0}\,\epsilon + \mathcal{O}(\epsilon^2)\ . \tag{1.201}$$

Note that Ω depends on the amplitude of the oscillations.

As an example, consider an oscillator with a quartic nonlinearity in the potential, *i.e.* $h(x) = r\,x^3$. Then

$$h\big(A\cos\theta\big) = \tfrac{3}{4}rA^3\,\cos\theta + \tfrac{1}{4}rA^3\,\cos(3\theta)\ . \tag{1.202}$$

We then obtain, setting $\epsilon = 1$ at the end of the calculation,

$$\Omega = \Omega_0 - \frac{3\,rA^2}{8\,\Omega_0} + \ldots \tag{1.203}$$

where the remainder is higher order in the amplitude A. In the case of the pendulum,

$$\ddot\theta + \Omega_0^2\,\theta = \tfrac{1}{6}\Omega_0^2\,\theta^3 + \mathcal{O}\big(\theta^5\big)\ , \tag{1.204}$$

and with $r = \frac{1}{6}\,\Omega_0^2$ and $\theta_0(t) = \theta_0\sin(\Omega t)$, we find

$$T(\theta_0) = \frac{2\pi}{\Omega} = \frac{2\pi}{\Omega_0}\cdot\Big\{1 + \tfrac{1}{16}\,\theta_0^2 + \ldots\Big\}\ . \tag{1.205}$$

One can check that this is correct to lowest nontrivial order in the amplitude, using the exact result for the period,

$$T(\theta_0) = \frac{4}{\Omega_0}\,\mathrm{K}\big(\sin^2\tfrac{1}{2}\theta_0\big)\ , \tag{1.206}$$

where $\mathrm{K}(x)$ is the complete elliptic integral.

The procedure can be continued to the next order, where the free parameter a_2 is used to eliminate resonant forcing terms on the RHS.

A good exercise to test one's command of the method is to work out the lowest order nontrivial corrections to the frequency of an oscillator with a cubic nonlinearity, such as $h(x) = rx^2$. One finds that there are no resonant forcing terms at first order in ϵ, hence one must proceed to second order to find the first nontrivial corrections to the frequency.

1.10 Multiple Time Scale Method

Another method of eliminating secular terms (*i.e.* driving terms which oscillate at the resonant frequency of the unperturbed oscillator), and one which has applicability beyond periodic motion alone, is that of multiple time scale analysis. Consider the equation

$$\ddot{x} + x = \epsilon\, h(x, \dot{x})\ , \tag{1.207}$$

where ϵ is presumed small, and $h(x, \dot{x})$ is a nonlinear function of position and/or velocity. We define a hierarchy of time scales: $t_n \equiv \epsilon^n\, t$. There is a normal time scale t_0, slow time scale t_1, a 'superslow' time scale t_1, *etc.* Thus,

$$\begin{aligned}\frac{d}{dt} &= \frac{\partial}{\partial t_0} + \epsilon\,\frac{\partial}{\partial t_1} + \epsilon^2\,\frac{\partial}{\partial t_2} + \ldots \\ &= \sum_{n=0}^{\infty} \epsilon^n\,\frac{\partial}{\partial t_n}\ .\end{aligned} \tag{1.208}$$

Next, we expand

$$x(t) = \sum_{n=0}^{\infty} \epsilon^n\, x_n(t, T)\ . \tag{1.209}$$

Thus, we have

$$\left(\sum_{n=0}^{\infty} \epsilon^n \frac{\partial}{\partial t_n}\right)^2 \left(\sum_{k=0}^{\infty} \epsilon^k\, x_k\right) + \sum_{k=0}^{\infty} \epsilon^k\, x_k = \epsilon\, h\left(\sum_{k=0}^{\infty} \epsilon^k\, x_k\ ,\ \sum_{n=0}^{\infty} \epsilon^n \frac{\partial}{\partial t_n}\left(\sum_{k=0}^{\infty} \epsilon^k\, x_k\right)\right)\ .$$

We now evaluate this order by order in ϵ:

$$\mathcal{O}(\epsilon^0) \;:\; \left(\frac{\partial^2}{\partial t_0^2}+1\right) x_0 = 0 \tag{1.210}$$

$$\mathcal{O}(\epsilon^1) \;:\; \left(\frac{\partial^2}{\partial t_0^2}+1\right) x_1 = -2\,\frac{\partial^2 x_0}{\partial t_0\,\partial t_1} + h\left(x_0, \frac{\partial x_0}{\partial t_0}\right) \tag{1.211}$$

$$\mathcal{O}(\epsilon^2) \;:\; \left(\frac{\partial^2}{\partial t_0^2}+1\right) x_2 = -2\,\frac{\partial^2 x_1}{\partial t_0\,\partial t_1} - 2\,\frac{\partial^2 x_0}{\partial t_0\,\partial t_2} - \frac{\partial^2 x_0}{\partial t_1^2} + \frac{\partial h}{\partial x}\bigg|_{\{x_0,\dot{x}_0\}} x_1 + \frac{\partial h}{\partial \dot{x}}\bigg|_{\{x_0,\dot{x}_0\}} \left(\frac{\partial x_1}{\partial t_0} + \frac{\partial x_0}{\partial t_1}\right) , \tag{1.212}$$

et cetera. The expansion gets more and more tedious with increasing order in ϵ.

Let's carry this procedure out to first order in ϵ. To order ϵ^0,

$$x_0 = A\,\cos\big(t_0+\phi\big)\ , \tag{1.213}$$

where A and ϕ are arbitrary (at this point) functions of $\{t_1, t_2, \ldots\}$. Now we solve the next equation in the hierarchy, for x_1. Let $\theta \equiv t_0 + \phi$. Then $\partial_{t_0} = \partial_\theta$ and we have

$$\left(\frac{\partial^2}{\partial\theta^2}+1\right) x_1 = 2\,\frac{\partial A}{\partial t_1}\,\sin\theta + 2\,A\,\frac{\partial\phi}{\partial t_1}\,\cos\theta + h\big(A\cos\theta, -A\sin\theta\big)\ . \tag{1.214}$$

Since the arguments of h are periodic under $\theta \to \theta + 2\pi$, we may expand h in a Fourier series:

$$h(\theta) \equiv h\big(A\cos\theta, -A\sin\theta\big) = \sum_{k=1}^{\infty} \alpha_k(A)\sin(k\theta) + \sum_{k=0}^{\infty} \beta_k(A)\cos(k\theta)\ . \tag{1.215}$$

The inverse of this relation is

$$\alpha_k(A) = \int_0^{2\pi} \frac{d\theta}{\pi}\,h(\theta)\,\sin(k\theta) \qquad (k>0) \tag{1.216}$$

$$\beta_0(A) = \int_0^{2\pi} \frac{d\theta}{2\pi}\,h(\theta) \tag{1.217}$$

$$\beta_k(A) = \int_0^{2\pi} \frac{d\theta}{\pi}\,h(\theta)\,\cos(k\theta) \qquad (k>0)\ . \tag{1.218}$$

We now demand that the secular terms on the RHS – those terms proportional to $\cos\theta$ and $\sin\theta$ – must vanish. This means

$$2\,\frac{\partial A}{\partial t_1} + \alpha_1(A) = 0 \tag{1.219}$$

$$2A\,\frac{\partial\phi}{\partial t_1} + \beta_1(A) = 0\ . \tag{1.220}$$

These two first order equations require two initial conditions, which is sensible since our initial equation $\ddot{x} + x = \epsilon\, h(x, \dot{x})$ is second order in time.

With the secular terms eliminated, we may solve for x_1:

$$x_1 = \sum_{k\neq 1}^{\infty} \left\{ \frac{\alpha_k(A)}{1-k^2}\, \sin(k\theta) + \frac{\beta_k(A)}{1-k^2}\, \cos(k\theta) \right\} + C_0 \cos(\theta + \eta_0)\ . \tag{1.221}$$

Note: (i) the $k = 1$ terms are excluded from the sum, and (ii) an arbitrary solution to the homogeneous equation, *i.e.* eqn. 1.214 with the right hand side set to zero, is included. The constants C_0 and η_0 are arbitrary functions of t_1, t_2, *etc.* .

The equations for A and ϕ are both first order in t_1. They will therefore involve two constants of integration – call them A_0 and ϕ_0. At second order, these constants are taken as dependent upon the superslow time scale t_2. *The method itself may break down at this order.* (See if you can find out why.)

Let's apply this to the nonlinear oscillator $\ddot{x} + \sin x = 0$, also known as the simple pendulum. We'll expand the sine function to include only the lowest order nonlinear term, and consider

$$\ddot{x} + x = \tfrac{1}{6}\,\epsilon\, x^3\ . \tag{1.222}$$

We'll assume ϵ is small and take $\epsilon = 1$ at the end of the calculation. This will work provided the amplitude of the oscillation is itself small. To zeroth order, we have $x_0 = A\,\cos(t + \phi)$, as always. At first order, we must solve

$$\begin{aligned}\left(\frac{\partial^2}{\partial\theta^2} + 1\right) x_1 &= 2\,\frac{\partial A}{\partial t_1}\,\sin\theta + 2\,A\,\frac{\partial\phi}{\partial t_1}\,\cos\theta + \tfrac{1}{6}\,A^2\cos^3\theta \\ &= 2\,\frac{\partial A}{\partial t_1}\,\sin\theta + 2\,A\,\frac{\partial\phi}{\partial t_1}\,\cos\theta + \tfrac{1}{24}\,A^3\,\cos(3\theta) + \tfrac{1}{8}\,A^3\,\cos\theta\ .\end{aligned} \tag{1.223}$$

We eliminate the secular terms by demanding

$$\frac{\partial A}{\partial t_1} = 0 \qquad , \qquad \frac{\partial\phi}{\partial t_1} = -\tfrac{1}{16}\,A^2\ , \tag{1.224}$$

hence $A = A_0$ and $\phi = -\frac{1}{16}\,A_0^2\,t_1 + \phi_0$, and

$$\begin{aligned}x(t) = A_0 \cos\left(t - \tfrac{1}{16}\,\epsilon\,A_0^2\,t + \phi_0\right) \\ - \tfrac{1}{192}\,\epsilon\,A_0^3\,\cos\left(3t - \tfrac{3}{16}\,\epsilon A_0^2\,t + 3\phi_0\right) + \ldots\ ,\end{aligned} \tag{1.225}$$

which reproduces the result obtained from the Poincaré-Lindstedt method.

1.10.1 Duffing Oscillator

Consider the equation

$$\ddot{x} + 2\epsilon\mu\dot{x} + x + \epsilon x^3 = 0\ . \tag{1.226}$$

This describes a damped nonlinear oscillator. Here we assume both the damping coefficient $\tilde{\mu} \equiv \epsilon\mu$ as well as the nonlinearity both depend linearly on the small parameter ϵ. We may write this equation in our standard form $\ddot{x} + x = \epsilon\, h(x, \dot{x})$, with $h(x, \dot{x}) = -2\mu\dot{x} - x^3$.

For $\epsilon > 0$, which we henceforth assume, it is easy to see that the only fixed point is $(x, \dot{x}) = (0, 0)$. The linearized flow in the vicinity of the fixed point is given by

$$\frac{d}{dt}\begin{pmatrix} x \\ \dot{x} \end{pmatrix} = \begin{pmatrix} 0 & 1 \\ -1 & -2\epsilon\mu \end{pmatrix}\begin{pmatrix} x \\ \dot{x} \end{pmatrix} + \mathcal{O}(x^3)\ . \tag{1.227}$$

The determinant is $D = 1$ and the trace is $T = -2\epsilon\mu$. Thus, provided $\epsilon\mu < 1$, the fixed point is a stable spiral; for $\epsilon\mu > 1$ the fixed point becomes a stable node.

We employ the multiple time scale method to order ϵ. We'll save some indices and write $\tau \equiv t_0 = t$ and $T \equiv t_1 = \epsilon t$. We have $x_0 = A\cos(\tau + \phi)$ to zeroth order, as usual. The nonlinearity is expanded in a Fourier series in $\theta = \tau + \phi$:

$$\begin{aligned} h\big(x_0\,,\,\partial_\tau x_0\big) &= 2\mu A\sin\theta - A^3\cos^3\theta \\ &= 2\mu A\sin\theta - \tfrac{3}{4}A^3\cos\theta - \tfrac{1}{4}A^3\cos 3\theta\ . \end{aligned} \tag{1.228}$$

Thus, $\alpha_1(A) = 2\mu A$ and $\beta_1(A) = -\frac{3}{4}A^3$. We now solve the first order equations,

$$\frac{\partial A}{\partial T} = -\tfrac{1}{2}\,\alpha_1(A) = -\mu A \qquad \Longrightarrow \qquad A(T) = A_0\, e^{-\mu T} \tag{1.229}$$

as well as

$$\frac{\partial\phi}{\partial T} = -\frac{\beta_1(A)}{2A} = \tfrac{3}{8}A_0^2\, e^{-2\mu T} \qquad \Longrightarrow \qquad \phi(T) = \phi_0 + \frac{3A_0^2}{16\mu}\left(1 - e^{-2\mu T}\right)\ . \tag{1.230}$$

After elimination of the secular terms, we may read off

$$x_1(\tau, T) = \tfrac{1}{32}A^3(T)\cos\big(3\tau + 3\phi(T)\big)\ . \tag{1.231}$$

Finally, we have

$$\begin{aligned} x(t) = A_0\, e^{-\epsilon\mu t}\,\cos\Big(t + \frac{3A_0^2}{16\mu}\left(1 - e^{-2\epsilon\mu t}\right) + \phi_0\Big) \\ + \tfrac{1}{32}\epsilon A_0^3\, e^{-3\epsilon\mu t}\,\cos\Big(3t + \frac{9A_0^2}{16\mu}\left(1 - e^{-2\epsilon\mu t}\right) + 3\phi_0\Big)\ . \end{aligned} \tag{1.232}$$

1.10.2 Forced Duffing Oscillator

The forced, damped linear oscillator,

$$\ddot{x} + 2\mu\dot{x} + x = f_0\cos\Omega t \tag{1.233}$$

has the solution

$$x(t) = x_{\rm h}(t) + C(\Omega)\,\cos\big(\Omega t + \delta(\Omega)\big)\ , \tag{1.234}$$

where

$$x_{\rm h}(t) = A_+\,e^{\lambda_+ t} + A_-\,e^{\lambda_- t}\ , \tag{1.235}$$

where $\lambda_\pm = -\mu \pm \sqrt{\mu^2 - 1}$ are the roots of $\lambda^2 + 2\mu\lambda + 1 = 0$. The 'susceptibility' C and phase shift δ are given by

$$C(\Omega) = \frac{1}{\sqrt{(\Omega^2-1)^2 + 4\mu^2\Omega^2}} \qquad , \qquad \delta(\Omega) = \tan^{-1}\left(\frac{2\mu\Omega}{1-\Omega^2}\right)\ . \tag{1.236}$$

The homogeneous solution, $x_{\rm h}(t)$, is a transient and decays exponentially with time, since $\mathrm{Re}(\lambda_\pm) < 0$. The asymptotic behavior is a phase-shifted oscillation at the driving frequency Ω.

Now let's add a nonlinearity. We study the equation

$$\ddot x + x = \epsilon\,h(x,\dot x) + \epsilon\,f_0\,\cos(t + \epsilon\nu t)\ . \tag{1.237}$$

Note that amplitude of the driving term, $\epsilon f_0\cos(\Omega t)$, is assumed to be small, *i.e.* proportional to ϵ, and the driving frequency $\Omega = 1 + \epsilon\nu$ is assumed to be close to resonance. (The resonance frequency of the unperturbed oscillator is $\omega_{\rm res} = 1$.) Were the driving frequency far from resonance, it could be dealt with in the same manner as the non-secular terms encountered thus far. The situation when Ω is close to resonance deserves our special attention.

At order ϵ^0, we still have $x_0 = A\cos(\tau+\phi)$, with $\tau = t$ and $T = \epsilon t$. At order ϵ^1, we must solve

$$\begin{aligned}\left(\frac{\partial^2}{\partial\theta^2} + 1\right)x_1 &= 2A'\sin\theta + 2A\phi'\cos\theta + h\big(A\cos\theta\ ,\ -A\sin\theta\big) + f_0\,\cos(\theta-\psi)\\ &= \sum_{k\neq 1}\Big(\alpha_k\sin(k\theta) + \beta_k\cos(k\theta)\Big) + \Big(2A' + \alpha_1 + f_0\sin\psi\Big)\sin\theta\\ &\qquad + \Big(2A\psi' + 2A\nu + \beta_1 + f_0\cos\psi\Big)\cos\theta\ ,\end{aligned} \tag{1.238}$$

where $\psi \equiv \phi(T) - \nu T$, and where the prime denotes differentiation with respect to T. We must therefore solve

$$\frac{dA}{dT} = -\tfrac{1}{2}\alpha_1(A) - \tfrac{1}{2}f_0\sin\psi \tag{1.239}$$

$$\frac{d\psi}{dT} = -\nu - \frac{\beta_1(A)}{2A} - \frac{f_0}{2A}\cos\psi\ . \tag{1.240}$$

If we assume that $\{A,\psi\}$ approaches a fixed point of these dynamics, then at the fixed point these equations provide a relation between the amplitude A, the 'detuning' parameter ν, and the drive f_0:

$$\Big[\alpha_1(A)\Big]^2 + \Big[2\nu A + \beta_1(A)\Big]^2 = f_0^2\ . \tag{1.241}$$

Thus far our approach has been completely general. We now restrict our attention to the Duffing equation, for which

$$\alpha_1(A) = 2\mu A \qquad , \qquad \beta_1(A) = -\tfrac{3}{4}A^3 \ , \tag{1.242}$$

which yields the cubic equation

$$A^6 - \tfrac{16}{3}\nu A^4 + \tfrac{64}{9}(\mu^2+\nu^2)A^2 - \tfrac{16}{9}f_0^2 = 0 \ . \tag{1.243}$$

Analyzing the cubic is a good exercise. Setting $y = A^2$, we define

$$G(y) \equiv y^3 - \tfrac{16}{3}\nu\, y^2 + \tfrac{64}{9}(\mu^2+\nu^2)\, y \ , \tag{1.244}$$

and we seek a solution to $G(y) = \frac{16}{9}f_0^2$. Setting $G'(y) = 0$, we find roots at

$$y_\pm = \tfrac{16}{9}\nu \pm \tfrac{8}{9}\sqrt{\nu^2 - 3\mu^2} \ . \tag{1.245}$$

Thus, $\nu\, y_\pm \geq 0$, and thus, since $y = A^2$ must be positive, there is a unique solution to $G(y) = \frac{16}{9}f_0^2$ for $\nu \in \big[-\infty, \sqrt{3}\,\mu\big]$, for all f_0.

For $\nu > \sqrt{3}\,\mu$, the function $G(y)$ has a local maximum at $y = y_-$ and a local minimum at $y = y_+$. There are then three solutions for $y(\nu)$ for $f_0 \in \big[f_0^-, f_0^+\big]$, where $f_0^\pm = \frac{3}{4}\sqrt{G(y_\mp)}$. If we define $\kappa \equiv \nu/\mu$, then

$$f_0^\pm = \tfrac{8}{9}\,\mu^{3/2}\sqrt{\kappa^3 + 9\kappa \pm \sqrt{\kappa^2-3}} \ . \tag{1.246}$$

The phase diagram is shown in Fig. 1.31. The minimum value for f_0 is $f_{0,\rm c} = \frac{16}{3^{5/4}}\,\mu^{3/2}$, which occurs at $\kappa = \sqrt{3}$.

Thus far we have assumed that the (A, ψ) dynamics evolves to a fixed point. We should check to make sure that this fixed point is in fact stable. To do so, we evaluate the linearized dynamics at the fixed point. Writing $A = A^* + \delta A$ and $\psi = \psi^* + \delta\psi$, we have

$$\frac{d}{dT}\begin{pmatrix}\delta A\\ \delta\psi\end{pmatrix} = M\begin{pmatrix}\delta A\\ \delta\psi\end{pmatrix} \ , \tag{1.247}$$

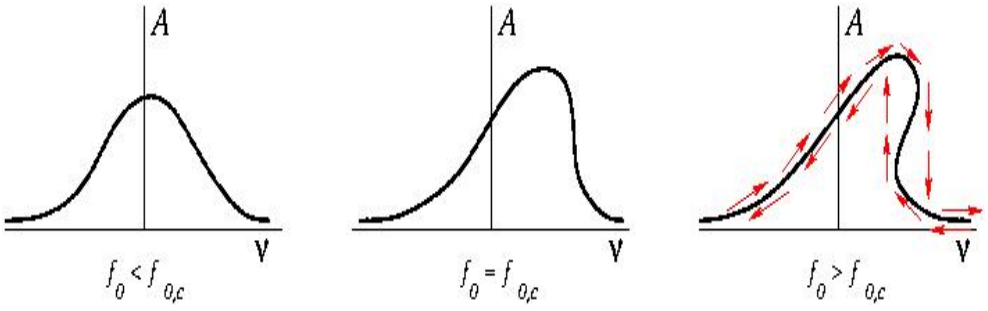

Figure 1.30: Amplitude A *versus* detuning ν for the forced Duffing oscillator for three values of the drive f_0. The critical drive is $f_{0,\rm c} = \frac{16}{3^{5/4}}\,\mu^{3/2}$. For $f_0 > f_{0,\rm c}$, there is hysteresis as a function of the detuning.

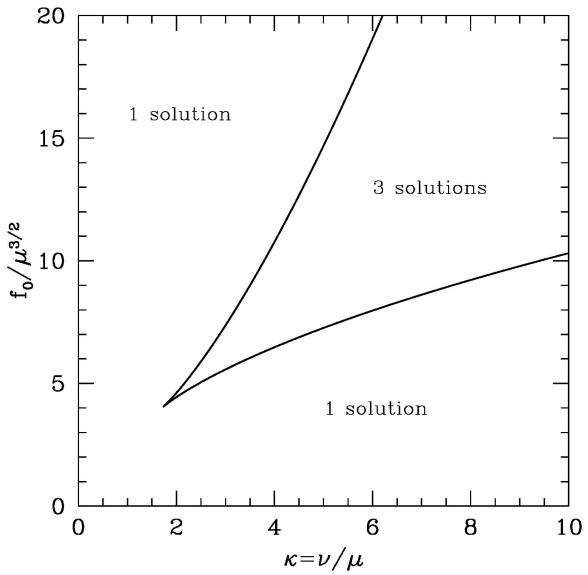

Figure 1.31: Phase diagram for the forced Duffing oscillator.

with

$$M = \begin{pmatrix} \frac{\partial \dot{A}}{\partial A} & \frac{\partial \dot{A}}{\partial \psi} \\ \\ \frac{\partial \dot{\psi}}{\partial A} & \frac{\partial \dot{\psi}}{\partial \psi} \end{pmatrix} = \begin{pmatrix} -\mu & -\frac{1}{2} f_0 \, \cos\psi \\ \\ \frac{3}{4}A + \frac{f_0}{2A^2} \, \cos\psi & \frac{f_0}{2A} \, \sin\psi \end{pmatrix}$$

$$= \begin{pmatrix} -\mu & \nu A - \frac{3}{8}A^3 \\ \\ \frac{9}{8}A - \frac{\nu}{A} & -\mu \end{pmatrix} \ . \tag{1.248}$$

One then has $T = -2\mu$ and

$$D = \mu^2 + \big(\nu - \tfrac{3}{8}A^2\big)\big(\nu - \tfrac{9}{8}A^2\big) \ . \tag{1.249}$$

Setting $D = \frac{1}{4}T^2 = \mu^2$ sets the boundary between stable spiral and stable node. Setting $D = 0$ sets the boundary between stable node and saddle. The fixed point structure is as shown in Fig. 1.32.

1.10.3 Van der Pol Oscillator

Let's apply this method to another problem, that of the van der Pol oscillator,

$$\ddot{x} + \epsilon\,(x^2 - 1)\,\dot{x} + x = 0 \ , \tag{1.250}$$

with $\epsilon > 0$. The nonlinear term acts as a frictional drag for $x > 1$, and as a 'negative friction' (*i.e.* increasing the amplitude) for $x < 1$. Note that the linearized equation at the fixed point $(x = 0, \dot{x} = 0)$ corresponds to an unstable spiral for $\epsilon < 2$.

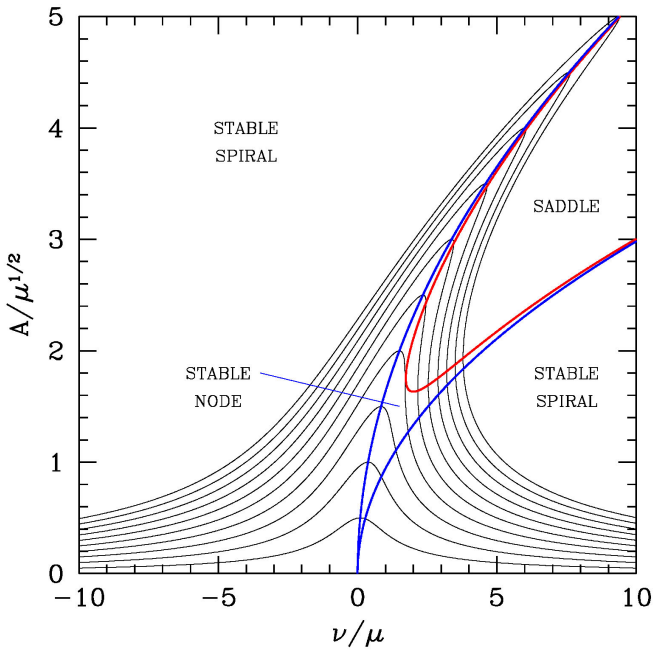

Figure 1.32: Amplitude *versus* detuning for the forced Duffing oscillator for ten equally spaced values of f_0 between $\mu^{3/2}$ and $10\,\mu^{3/2}$. The critical value is $f_{0,c} = 4.0525\,\mu^{3/2}$. The red and blue curves are boundaries for the fixed point classification.

For the van der Pol oscillator, we have $h(x,\dot{x}) = (1-x^2)\,\dot{x}$, and plugging in the zeroth order solution $x_0 = A\,\cos(t+\phi)$ gives

$$h\left(x_0\,,\,\frac{\partial x_0}{\partial t_0}\right) = \big(1 - A^2\cos^2\theta\big)\,\big(-A\sin\theta\big)$$
$$= \big(-A + \tfrac{1}{4}A^3\big)\,\sin\theta + \tfrac{1}{4}\,A^3\,\sin(3\theta)\;, \tag{1.251}$$

with $\theta \equiv t+\phi$. Thus, $\alpha_1 = -A + \frac{1}{4}A^3$ and $\beta_1 = 0$, which gives $\phi = \phi_0$ and

$$2\,\frac{\partial A}{\partial t_1} = A - \tfrac{1}{4}A^3\;. \tag{1.252}$$

The equation for A is easily integrated:

$$dt_1 = -\frac{8\,dA}{A\,(A^2-4)} = \left(\frac{2}{A} - \frac{1}{A-2} - \frac{1}{A+2}\right)dA = d\ln\left(\frac{A}{A^2-4}\right)$$
$$\implies \qquad A(t_1) = \frac{2}{\sqrt{1 - \big(1-\frac{4}{A_0^2}\big)\exp(-t_1)}}\;. \tag{1.253}$$

Thus,

$$x_0(t) = \frac{2\,\cos(t+\phi_0)}{\sqrt{1 - \big(1-\frac{4}{A_0^2}\big)\exp(-\epsilon t)}}\;. \tag{1.254}$$

This behavior describes the approach to the limit cycle $\cos(t+\phi_0)$. With the elimination of the secular terms, we have

$$x_1(t) = -\tfrac{1}{32}A^3\sin(3\theta) = -\frac{\frac{1}{4}\sin\big(3t+3\phi_0\big)}{\left[1-\big(1-\frac{4}{A_0^2}\big)\exp(-\epsilon t)\right]^{3/2}}\ . \tag{1.255}$$

1.10.4 Forced van der Pol Oscillator

Consider now a weakly dissipative, weakly forced van der Pol oscillator, governed by the equation

$$\ddot{x} + \epsilon\,(x^2-1)\,\dot{x} + x = \epsilon\, f_0\,\cos(t+\epsilon\nu t)\ , \tag{1.256}$$

where the forcing frequency is $\Omega = 1+\epsilon\nu$, which is close to the natural frequency $\omega_0 = 1$. We apply the multiple time scale method, with $h(x,\dot{x}) = (1-x^2)\,\dot{x}$. As usual, the lowest order solution is $x_0 = A(T)\cos\big(\tau+\phi(T)\big)$, where $\tau = t$ and $T = \epsilon t$. Again, we define $\theta \equiv \tau + \phi(T)$ and $\psi(T) \equiv \phi(T) - \nu T$. From

$$h(A\cos\theta, -A\sin\theta) = \big(\tfrac{1}{4}A^3 - A\big)\,\sin\theta + \tfrac{1}{4}A^3\sin(3\theta)\ , \tag{1.257}$$

we arrive at

$$\begin{aligned}\left(\frac{\partial^2}{\partial\theta^2}+1\right)x_1 &= -2\frac{\partial^2 x_0}{\partial\tau\,\partial T} + h\left(x_0, \frac{\partial x_0}{\partial\tau}\right)\\ &= \big(\tfrac{1}{4}A^3 - A + 2A' + f_0\sin\psi\big)\sin\theta\\ &\quad + \big(2A\,\psi' + 2\nu A + f_0\cos\psi\big)\cos\theta + \tfrac{1}{4}A^3\sin(3\theta)\ .\end{aligned} \tag{1.258}$$

We eliminate the secular terms, proportional to $\sin\theta$ and $\cos\theta$, by demanding

$$\frac{dA}{dT} = \tfrac{1}{2}A - \tfrac{1}{8}A^3 - \tfrac{1}{2}f_0\sin\psi \tag{1.259}$$

$$\frac{d\psi}{dT} = -\nu - \frac{f_0}{2A}\cos\psi\ . \tag{1.260}$$

Stationary solutions have $A' = \psi' = 0$, hence $\cos\psi = -2\nu\,A/f_0$, and hence

$$\begin{aligned}f_0^2 &= 4\nu^2A^2 + \big(1+\tfrac{1}{4}A^2\big)^2A^2\\ &= \tfrac{1}{16}A^6 - \tfrac{1}{2}A^4 + (1+4\nu^2)A^2\ .\end{aligned} \tag{1.261}$$

For this solution, we have

$$x_0 = A^*\cos(\tau+\nu T+\psi^*)\ , \tag{1.262}$$

and the oscillator's frequency is the forcing frequency Ω. This oscillator is thus *entrained*.

To proceed further, let $y = A^2$, and consider the cubic equation

$$F(y) = \tfrac{1}{16}y^3 - \tfrac{1}{2}y^2 + (1+4\nu^2)\,y - f_0^2 = 0\ . \tag{1.263}$$

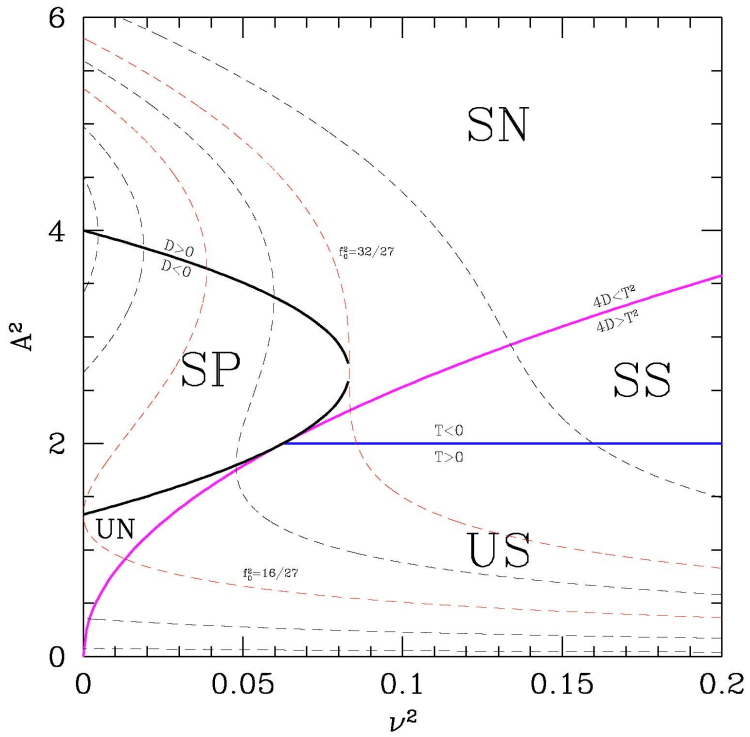

Figure 1.33: Amplitude *versus* detuning for the forced van der Pol oscillator. Fixed point classifications are abbreviated SN (stable node), SS (stable spiral), UN (unstable node), US (unstable spiral), and SP (saddle point).

Setting $F'(y) = 0$, we find the roots of $F'(y)$ lie at $y_\pm = \frac{4}{3}\,(2 \pm u)$, where $u = (1 - 12\,\nu^2)^{1/2}$. Thus, the roots are complex for $\nu^2 > \frac{1}{12}$, in which case $F(y)$ is monotonically increasing, and there is a unique solution to $F(y) = 0$. Since $F(0) = -f_0^2 < 0$, that solution satisfies $y > 0$. For $\nu^2 < \frac{1}{12}$, there are two local extrema at $y = y_\pm$. When $F_{\rm min} = F(y_+) < 0 < F(y_-) = F_{\rm max}$, the cubic $F(y)$ has three real, positive roots. This is equivalent to the condition

$$-\tfrac{8}{27}\,u^3 + \tfrac{8}{9}\,u^2 < \tfrac{32}{27} - f_0^2 < \tfrac{8}{27}\,u^3 + \tfrac{8}{9}\,u^2 \ . \tag{1.264}$$

We can say even more by exploring the behavior of (1.33,1.34) in the vicinity of the fixed points. Writing $A = A^* + \delta A$ and $\psi = \psi^* + \delta\psi$, we have

$$\begin{pmatrix} d_T\,\delta A \\ \\ d_T\,\delta\psi \end{pmatrix} = \begin{pmatrix} \frac{1}{2}\big(1 - \frac{3}{4}A^{*2}\big) & \nu A^* \\ \\ -\nu/A^* & \frac{1}{2}\big(1 - \frac{1}{4}A^{*2}\big) \end{pmatrix} \begin{pmatrix} \delta A \\ \\ \delta\psi \end{pmatrix} \ . \tag{1.265}$$

The eigenvalues of the linearized dynamics at the fixed point are given by $\lambda_\pm = \frac{1}{2}\big(T \pm \sqrt{T^2 - 4D}\big)$, where T and D are the trace and determinant of the linearized equation. Recall now the classification scheme for fixed points of two-dimensional phase flows, discussed in section 1.5.1. To recapitulate, when $D < 0$, we have $\lambda_- < 0 < \lambda_+$ and the fixed point is

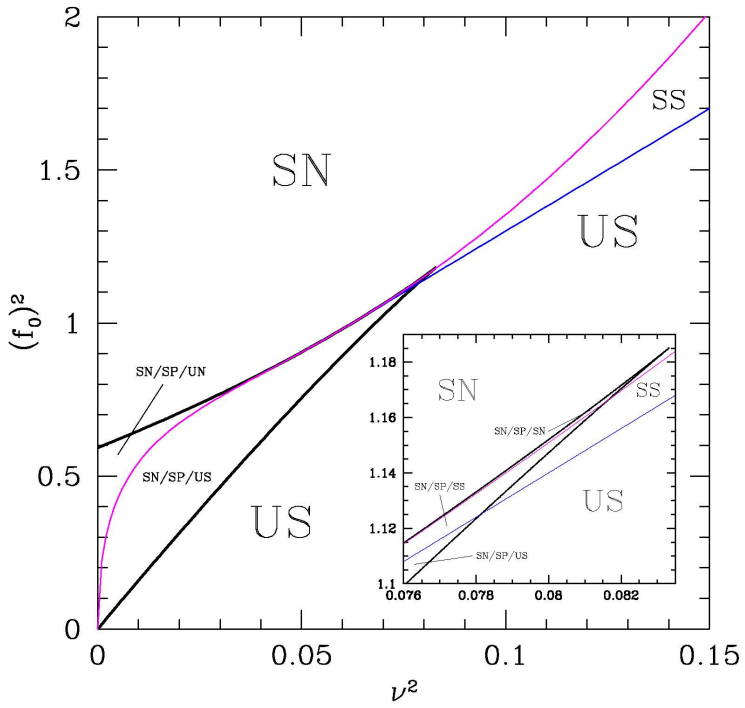

Figure 1.34: Phase diagram for the weakly forced van der Pol oscillator in the (ν^2, f_0^2) plane. Inset shows detail. Abbreviations for fixed point classifications are as in Fig. 1.33.

a saddle. For $0 < 4D < T^2$, both eigenvalues have the same sign, so the fixed point is a node. For $4D > T^2$, the eigenvalues form a complex conjugate pair, and the fixed point is a spiral. A node/spiral fixed point is stable if $T < 0$ and unstable if $T > 0$. For our forced van der Pol oscillator, we have

$$T = 1 - \tfrac{1}{2}A^{*2} \tag{1.266}$$

$$D = \tfrac{1}{4}\big(1 - A^{*2} + \tfrac{3}{16}A^{*4}\big) + \nu^2 \ . \tag{1.267}$$

From these results we can obtain the plot of Fig. 1.33, where amplitude is shown *versus* detuning. Note that for $f_0 < \sqrt{\frac{32}{27}}$ there is a region $\big[\nu_-, \nu_+\big]$ of hysteretic behavior in which varying the detuning parameter ν is not a reversible process. The phase diagram in the (ν^2, f_0^2) is shown in Fig. 1.34.

Finally, we can make the following statement about the *global* dynamics (*i.e.* not simply in the vicinity of a fixed point). For large A, we have

$$\frac{dA}{dT} = -\tfrac{1}{8}A^3 + \ldots \qquad , \qquad \frac{d\psi}{dT} = -\nu + \ldots \ . \tag{1.268}$$

This flow is inward, hence if the flow is not to a stable fixed point, it must be attracted to a limit cycle. The limit cycle necessarily involves several frequencies. This result – the generation of new frequencies by nonlinearities – is called *heterodyning.*

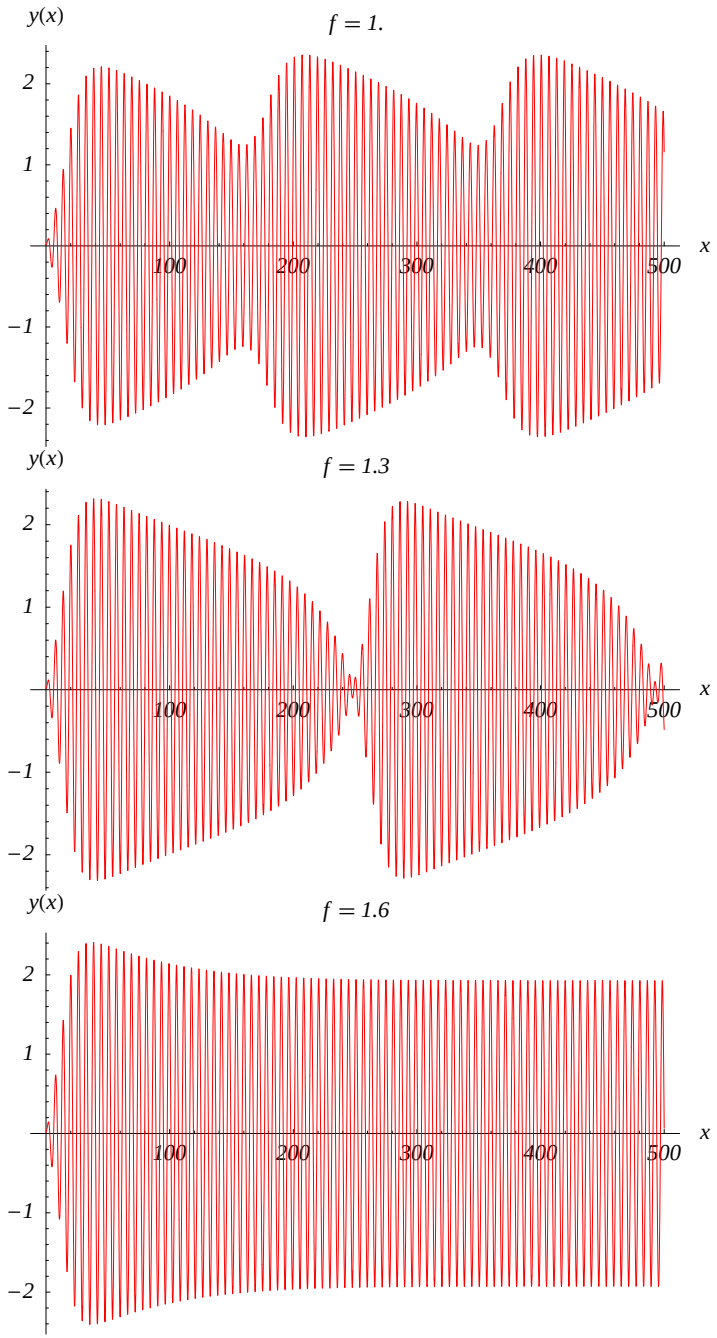

Figure 1.35: Forced van der Pol system with $\epsilon = 0.1$, $\nu = 0.4$ for three values of f_0. The limit entrained solution becomes unstable at $f_0 = 1.334$.

We can see heterodyning in action in the van der Pol system. In Fig. 1.34, the blue line which separates stable and unstable spiral solutions is given by $f_0^2 = 8\nu^2 + \frac{1}{2}$. For

example, if we take $\nu = 0.40$ then the boundary lies at $f_0 = 1.334$. For $f_0 < 1.334$, we expect heterodyning, as the entrained solution is unstable. For $f > 1.334$ the solution is entrained and oscillates at a fixed frequency. This behavior is exhibited in Fig. 1.35.

1.10.5 Relaxation Oscillations

We saw how to use multiple time scale analysis to identify the limit cycle of the van der Pol oscillator when ϵ is small. Consider now the opposite limit, where the coefficient of the damping term is very large. We generalize the van der Pol equation to

$$\ddot{x} + \mu\,\Phi(x)\,\dot{x} + x = 0 \ , \tag{1.269}$$

and suppose $\mu \gg 1$. Define now the variable

$$\begin{aligned} y &\equiv \frac{\dot{x}}{\mu} + \int_0^x dx'\,\Phi(x') \\ &= \frac{\dot{x}}{\mu} + F(x) \ , \end{aligned} \tag{1.270}$$

where $F'(x) = \Phi(x)$. (y is sometimes called the *Liènard variable*, and (x, y) the *Liènard plane*.) Then the original second order equation may be written as two coupled first order equations:

$$\dot{y} = -\frac{x}{\mu} \tag{1.271}$$

$$\dot{x} = \mu\Big(y - F(x)\Big) \ . \tag{1.272}$$

Since $\mu \gg 1$, the first of these equations is *slow* and the second one *fast*. The dynamics rapidly achieves $y \approx F(x)$, and then slowly evolves along the curve $y = F(x)$, until it is forced to make a large, fast excursion.

A concrete example is useful. Consider $F(x)$ of the form sketched in Fig. 1.36. This is what one finds for the van der Pol oscillator, where $\Phi(x) = x^2 - 1$ and $F(x) = \frac{1}{3}x^3 - x$. The limit cycle behavior $x_{\rm LC}(t)$ is sketched in Fig. 1.37. We assume $\Phi(x) = \Phi(-x)$ for simplicity.

When $\mu \gg 1$ we can determine approximately the period of the limit cycle. Assuming $y = F(x)$ throughout the slow portion of the cycle, we have

$$\dot{y} = F'(x)\,\dot{x} = -\frac{x}{\mu} \qquad \Longrightarrow \qquad dt = -\mu\,\Phi(x)\,\frac{dx}{x} \ . \tag{1.273}$$

The period is then

$$T \simeq 2\mu \int_a^b dx\,\frac{\Phi(x)}{x} \ , \tag{1.274}$$

where $F'(\pm a) = \Phi(\pm a) = 0$ and $F(\pm b) = F(\mp a)$. For the van der Pol oscillator, with $\Phi(x) = x^2 - 1$, we have $a = 1$, $b = 2$, and $T \simeq (3 - 2\ln 2)\,\mu$.

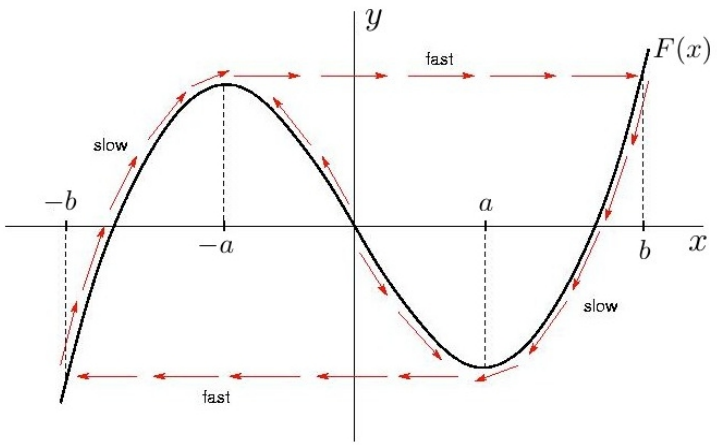

Figure 1.36: Relaxation oscillations in the so-called Lièнard plane. The system rapidly flows to a point on the curve $y = F(x)$, and then crawls slowly along this curve. The slow motion takes x from $-b$ to $-a$, after which the system executes a rapid jump to $x = +b$, then a slow retreat to $x = +a$, followed by a rapid drop to $x = -b$.

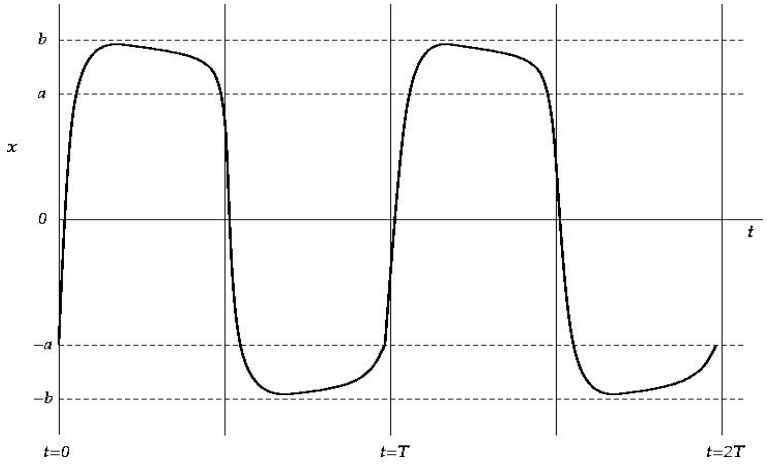

Figure 1.37: A sketch of he limit cycle for the relaxation oscillation studied in this section.

1.11 Parametric Oscillator

Consider the equation

$$\ddot{x} + \omega_0^2(t)\, x = 0 \ , \tag{1.275}$$

where the oscillation frequency is a function of time. Equivalently,

$$\frac{d}{dt}\begin{pmatrix} x \\ \dot{x} \end{pmatrix} = \overbrace{\begin{pmatrix} 0 & 1 \\ -\omega_0^2(t) & 0 \end{pmatrix}}^{M(t)} \overbrace{\begin{pmatrix} x \\ \dot{x} \end{pmatrix}}^{\varphi(t)} \ . \tag{1.276}$$

The formal solution is the path-ordered exponential,

$$\boldsymbol{\varphi}(t) = \mathcal{P} \exp\left\{ \int_0^t dt' \, M(t') \right\} \boldsymbol{\varphi}(0) \ . \tag{1.277}$$

Let's consider an example in which

$$\omega(t) = \begin{cases} (1+\epsilon)\,\omega_0 & \text{if } 2n\tau \le t \le (2n+1)\tau \\ \\ (1-\epsilon)\,\omega_0 & \text{if } (2n+1)\tau \le t \le (2n+2)\tau \ . \end{cases} \tag{1.278}$$

Define $\boldsymbol{\varphi}_n \equiv \boldsymbol{\varphi}(2n\tau)$. Then

$$\boldsymbol{\varphi}_{n+1} = \exp(M_-\tau)\, \exp(M_+\tau)\, \boldsymbol{\varphi}_n \ , \tag{1.279}$$

where

$$M_\pm = \begin{pmatrix} 0 & 1 \\ -\omega_\pm^2 & 0 \end{pmatrix} \ , \tag{1.280}$$

with $\omega_\pm \equiv (1 \pm \epsilon)\,\omega_0$. Note that $M_\pm^2 = -\omega_\pm^2 \cdot \mathbf{1}$ is a multiple of the identity. Evaluating the Taylor series for the exponential, one finds

$$\exp(M_\pm t) = \begin{pmatrix} \cos\omega_\pm\tau & \omega_\pm^{-1}\sin\omega_\pm\tau \\ -\omega_\pm\,\sin\omega_\pm\tau & \cos\omega_\pm\tau \end{pmatrix} \ , \tag{1.281}$$

from which we derive

$$\mathcal{Q} \equiv \begin{pmatrix} a & b \\ c & d \end{pmatrix} = \exp(M_-\tau)\, \exp(M_+\tau) \tag{1.282}$$

$$= \begin{pmatrix} \cos\omega_-\tau & \omega_-^{-1}\sin\omega_-\tau \\ -\omega_-\,\sin\omega_-\tau & \cos\omega_-\tau \end{pmatrix} \begin{pmatrix} \cos\omega_+\tau & \omega_+^{-1}\sin\omega_+\tau \\ -\omega_+\,\sin\omega_+\tau & \cos\omega_+\tau \end{pmatrix}$$

with

$$a = \cos\omega_-\tau\, \cos\omega_+\tau - \frac{\omega_+}{\omega_-}\, \sin\omega_-\tau\, \sin\omega_+\tau \tag{1.283}$$

$$b = \frac{1}{\omega_+}\, \cos\omega_-\tau \sin\omega_+\tau + \frac{1}{\omega_-}\, \sin\omega_-\tau \cos\omega_+\tau \tag{1.284}$$

$$c = -\omega_+\, \cos\omega_-\tau \sin\omega_+\tau - \omega_-\, \sin\omega_-\tau \cos\omega_+\tau \tag{1.285}$$

$$d = \cos\omega_-\tau\, \cos\omega_+\tau - \frac{\omega_-}{\omega_+}\, \sin\omega_-\tau\, \sin\omega_+\tau \ . \tag{1.286}$$

Note that $\det \exp(M_\pm\tau) = 1$, hence $\det\mathcal{Q} = 1$. Also note that

$$P(\lambda) = \det\big(\mathcal{Q} - \lambda \cdot \mathbf{1}\big) = \lambda^2 - T\lambda + \Delta \ , \tag{1.287}$$

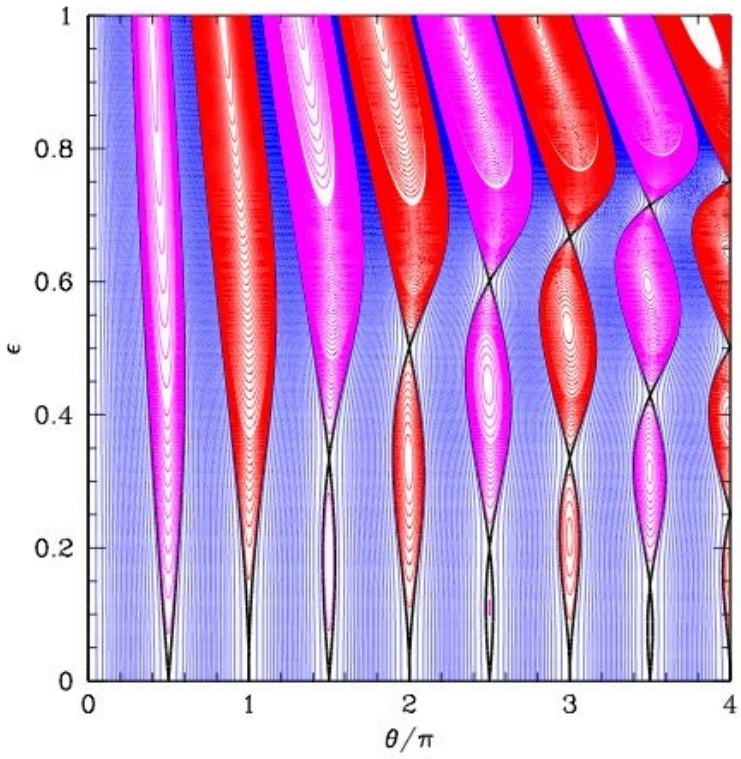

Figure 1.38: Phase diagram for the parametric oscillator in the (θ, ϵ) plane. Thick black lines correspond to $T = \pm 2$. Blue regions: $|T| < 2$. Red regions: $T > 2$. Magenta regions: $T < -2$.

where

$$T = a + d = \mathrm{Tr}\,\mathcal{Q} \tag{1.288}$$

$$\Delta = ad - bc = \det\mathcal{Q}\ . \tag{1.289}$$

The eigenvalues of $\mathcal{Q}$ are

$$\lambda_\pm = \tfrac{1}{2}T \pm \tfrac{1}{2}\sqrt{T^2 - 4\Delta}\ . \tag{1.290}$$

In our case, $\Delta = 1$. There are two cases to consider:

$$|T| < 2 : \lambda_+ = \lambda_-^* = e^{i\delta} \quad , \quad \delta = \cos^{-1}\tfrac{1}{2}T \tag{1.291}$$

$$|T| > 2 : \lambda_+ = \lambda_-^{-1} = \pm e^{\mu} \quad , \quad \mu = \cosh^{-1}\tfrac{1}{2}|T|\ . \tag{1.292}$$

When $|T| < 2$, $\boldsymbol{\varphi}$ remains bounded; when $|T| > 2$, $|\boldsymbol{\varphi}|$ increases exponentially with time. Note that phase space volumes are preserved by the dynamics.

To investigate more fully, let $\theta \equiv \omega_0\tau$. The period of the ω_0 oscillations is $\delta t = 2\tau$, *i.e.* $\omega_{\rm pump} = \pi/\tau$ is the frequency at which the system is 'pumped'. We compute the trace of

$\mathcal{Q}$ and find

$$\tfrac{1}{2}T = \frac{\cos(2\theta) - \epsilon^2\cos(2\epsilon\theta)}{1-\epsilon^2} \ . \tag{1.293}$$

We are interested in the boundaries in the (θ, ϵ) plane where $|T| = 2$. Setting $T = +2$, we write $\theta = n\pi + \delta$, which means $\omega_0 \approx n\omega_{\rm pump}$. Expanding for small δ and ϵ, we obtain the relation

$$\delta^2 = \epsilon^4\,\theta^2 \quad \Rightarrow \quad \epsilon = \left|\frac{\delta}{n\pi}\right|^{1/2} \ . \tag{1.294}$$

Setting $T = -2$, we write $\theta = (n + \frac{1}{2})\pi + \delta$, *i.e.* $\omega_0 \approx (n + \frac{1}{2})\,\omega_{\rm pump}$. This gives

$$\delta^2 = \epsilon^2 \quad \Rightarrow \quad \epsilon = \pm\delta \ . \tag{1.295}$$

The full phase diagram in the (θ, ϵ) plane is shown in Fig. 1.38. A physical example is pumping a swing. By extending your legs periodically, you effectively change the length $\ell(t)$ of the pendulum, resulting in a time-dependent $\omega_0(t) = \sqrt{g/\ell(t)}$.

1.12 Strange Attractors and Chaos : A Preview

An *attractor* of a dynamical system $\dot{\boldsymbol{\varphi}} = \boldsymbol{V}(\boldsymbol{\varphi})$ is the set of $\boldsymbol{\varphi}$ values that the system evolves to after a sufficiently long time. For $N = 1$ the only possible attractors are stable fixed points. For $N = 2$, we have stable notes and spirals, but also stable limit cycles. For $N > 3$ the situation is qualitatively different, and a fundamentally new type of set, the *strange attractor,* emerges.

A strange attractor is basically a bounded set on which nearby orbits diverge exponentially (*i.e.* there exists at least one positive Lyapunov exponent). To envision such a set, consider a flat rectangle, like a piece of chewing gum. Now fold the rectangle over, stretch it, and squash it so that it maintains its original volume. Keep doing this. Two points which started out nearby to each other will eventually, after a sufficiently large number of folds and stretches, grow far apart. Formally, a strange attractor is a *fractal*, and may have *noninteger Hausdorff dimension.* (We won't discuss fractals and Hausdorff dimension here.)

The canonical example of an $N = 3$ strange attractor is found in the Lorenz model. E. N. Lorenz, in a seminal paper from the early 1960's, reduced the essential physics of the coupled *partial* differential equations describing Rayleigh-Benard convection (a fluid slab of finite thickness, heated from below – in Lorenz's case a model of the atmosphere warmed by the ocean) to a set of twelve coupled nonlinear *ordinary* differential equations. Lorenz's intuition was that his weather model should exhibit recognizable patterns over time. What he found instead was that in some cases, changing his initial conditions by a part in a thousand rapidly led to totally different behavior. This *sensitive dependence on initial conditions* is a hallmark of chaotic systems.

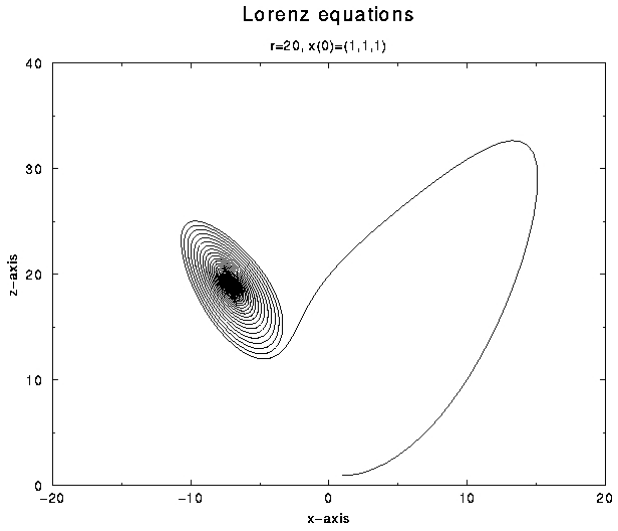

Figure 1.39: Evolution of the Lorenz equations for $\sigma = 10$, $b = \frac{8}{3}$, and $r = 20$, with initial conditions $(x, y, z) = (1, 1, 1)$, projected onto the (x, z) plane. The system is attracted by a stable spiral.

The essential physics (or mathematics?) of Lorenz's $N = 12$ system is elicited by the reduced $N = 3$ system,

$$\dot{X} = -\sigma X + \sigma Y \tag{1.296}$$

$$\dot{Y} = rX - Y - XZ \tag{1.297}$$

$$\dot{Z} = XY - bZ \ , \tag{1.298}$$

where σ, r, and b are all real and positive. Here t is the familiar time variable (appropriately scaled), and (X, Y, Z) represent linear combinations of physical fields, such as global wind current and poleward temperature gradient. These equations possess a symmetry under $(X, Y, Z) \to (-X, -Y, Z)$, but what is most important is the presence of nonlinearities in the second and third equations.

The Lorenz system is *dissipative* because phase space volumes contract:

$$\boldsymbol{\nabla} \cdot \boldsymbol{V} = \frac{\partial \dot{X}}{\partial X} + \frac{\partial \dot{Y}}{\partial Y} + \frac{\partial \dot{Z}}{\partial Z} = -(\sigma + b + 1) \ . \tag{1.299}$$

Thus, volumes contract under the flow. Another property is the following. Let

$$F(X, Y, Z) = \tfrac{1}{2}X^2 + \tfrac{1}{2}Y^2 + \tfrac{1}{2}(Z - r - \sigma)^2 \ . \tag{1.300}$$

Then

$$\begin{aligned} \dot{F} &= X\dot{X} + Y\dot{Y} + (Z - r - \sigma)\dot{Z} \\ &= -\sigma X^2 - Y^2 - b\big(Z - \tfrac{1}{2}r - \tfrac{1}{2}\sigma\big)^2 + \tfrac{1}{4}b(r + \sigma)^2 \ . \end{aligned} \tag{1.301}$$

Thus, $\dot{F} < 0$ outside an ellipsoid, which means that all solutions must remain bounded in phase space for all times.

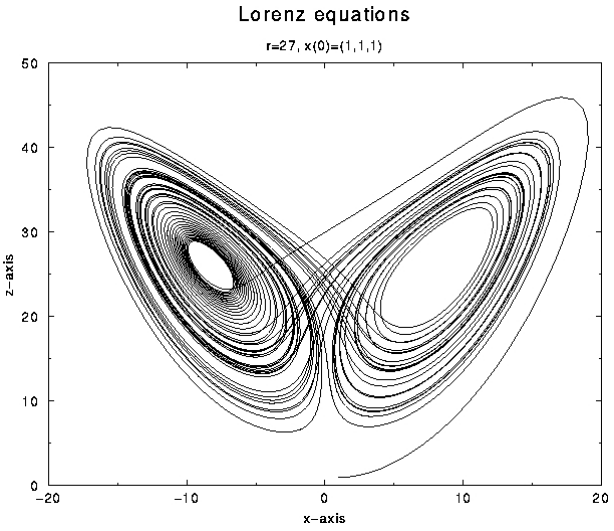

Figure 1.40: Evolution of the Lorenz equations for $\sigma = 10$, $b = \frac{8}{3}$, and $r = 28$, with initial conditions $(X_0, Y_0, Z_0) = (1, 1, 1)$, showing the 'strange attractor'.

1.12.1 Fixed Point Analysis

Setting $\dot{x} = \dot{y} = \dot{z} = 0$, we have three possible solutions. One solution, which is always present, is $x^* = y^* = z^* = 0$. If we linearize about this solution, we obtain

$$\frac{d}{dt}\begin{pmatrix}\delta X\\ \delta Y\\ \delta Z\end{pmatrix} = \begin{pmatrix}-\sigma & \sigma & 0\\ r & -1 & 0\\ 0 & 0 & -b\end{pmatrix}\begin{pmatrix}\delta X\\ \delta Y\\ \delta Z\end{pmatrix} \ . \tag{1.302}$$

The eigenvalues of the linearized dynamics are found to be

$$\begin{aligned}\lambda_{1,2} &= -\tfrac{1}{2}(1+\sigma) \pm \tfrac{1}{2}\sqrt{(1+\sigma)^2 + 4\sigma(r-1)} \\ \lambda_3 &= -b \ ,\end{aligned} \tag{1.303}$$

and thus if $0 < r < 1$ all three eigenvalues are negative, and the fixed point is a stable node. If, however, $r > 1$, then $\lambda_3 > 0$ and the fixed point is attractive in two directions but repulsive in a third, corresponding to a three-dimensional version of a saddle point.

For $r > 1$, a new pair of solutions emerges, with

$$X^* = Y^* = \pm\sqrt{b(r-1)} \quad , \quad Z^* = r - 1 \ . \tag{1.304}$$

Linearizing about either one of these fixed points, we find

$$\frac{d}{dt}\begin{pmatrix}\delta X\\ \delta Y\\ \delta Z\end{pmatrix} = \begin{pmatrix}-\sigma & \sigma & 0\\ 1 & -1 & -X^*\\ X^* & X^* & -b\end{pmatrix}\begin{pmatrix}\delta X\\ \delta Y\\ \delta Z\end{pmatrix} \ . \tag{1.305}$$

The characteristic polynomial of the linearized map is

$$P(\lambda) = \lambda^3 + (b + \sigma + 1)\,\lambda^2 + b(\sigma + r)\,\lambda + 2b(r-1) \ . \tag{1.306}$$

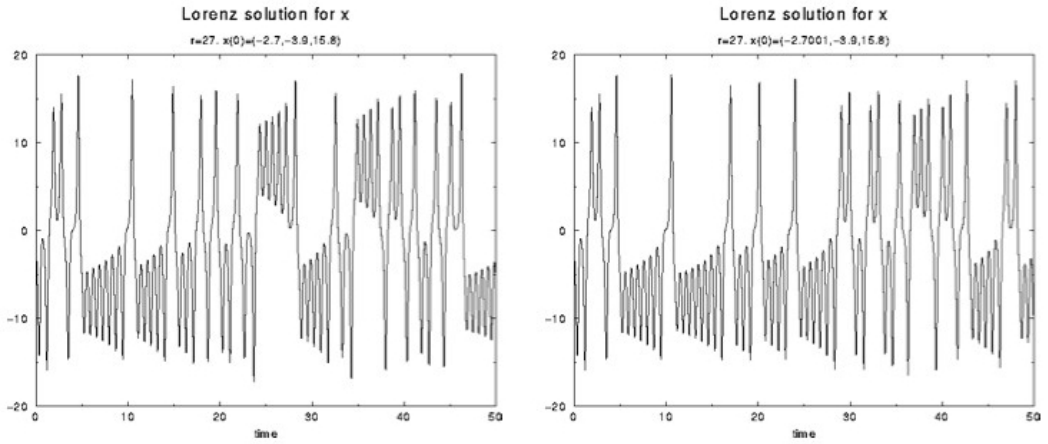

Figure 1.41: $X(t)$ for the Lorenz equations with $\sigma = 10$, $b = \frac{8}{3}$, $r = 28$, and initial conditions $(X_0, Y_0, Z_0) = (-2.7, -3.9, 15.8)$, and initial conditions $(X_0, Y_0, Z_0) = (-2.7001, -3.9, 15.8)$.

Since b, σ, and r are all positive, $P'(\lambda) > 0$ for all $\lambda \geq 0$. Since $P(0) = 2b(r-1) > 0$, we may conclude that there is always at least one eigenvalue λ_1 which is real and negative. The remaining two eigenvalues are either both real and negative, or else they occur as a complex conjugate pair: $\lambda_{2,3} = \alpha \pm i\beta$. The fixed point is stable provided $\alpha < 0$. The stability boundary lies at $\alpha = 0$. Thus, we set

$$P(i\beta) = \Big[2b(r-1) - (b+\sigma+1)\beta^2\Big] + i\Big[b(\sigma+r) - \beta^2\Big]\beta = 0 \ , \tag{1.307}$$

which results in two equations. Solving these two equations for $r(\sigma, b)$, we find

$$r_{\rm c} = \frac{\sigma(\sigma+b+3)}{\sigma-b-1} \ . \tag{1.308}$$

The fixed point is stable for $r \in \big[1, r_{\rm c}\big]$. These fixed points correspond to steady convection. The approach to this fixed point is shown in Fig. 1.39.

The Lorenz system has commonly been studied with $\sigma = 10$ and $b = \frac{8}{3}$. This means that the volume collapse is very rapid, since $\boldsymbol{\nabla} \cdot \boldsymbol{V} = -\frac{41}{3} \approx -13.67$, leading to a volume contraction of $e^{-41/3} \simeq 1.16 \times 10^{-6}$ per unit time. For these parameters, one also has $r_{\rm c} = \frac{470}{19} \approx 24.74$. The capture by the strange attractor is shown in Fig. 1.40.

In addition to the new pair of fixed points, a strange attractor appears for $r > r_{\rm s} \simeq 24.06$. In the narrow interval $r \in [24.06, 24.74]$ there are then *three* stable attractors, two of which correspond to steady convection and the third to chaos. Over this interval, there is also hysteresis. *I.e.* starting with a convective state for $r < 24.06$, the system remains in the convective state until $r = 24.74$, when the convective fixed point becomes unstable. The system is then driven to the strange attractor, corresponding to chaotic dynamics. Reversing the direction of r, the system remains chaotic until $r = 24.06$, when the strange attractor loses its own stability.

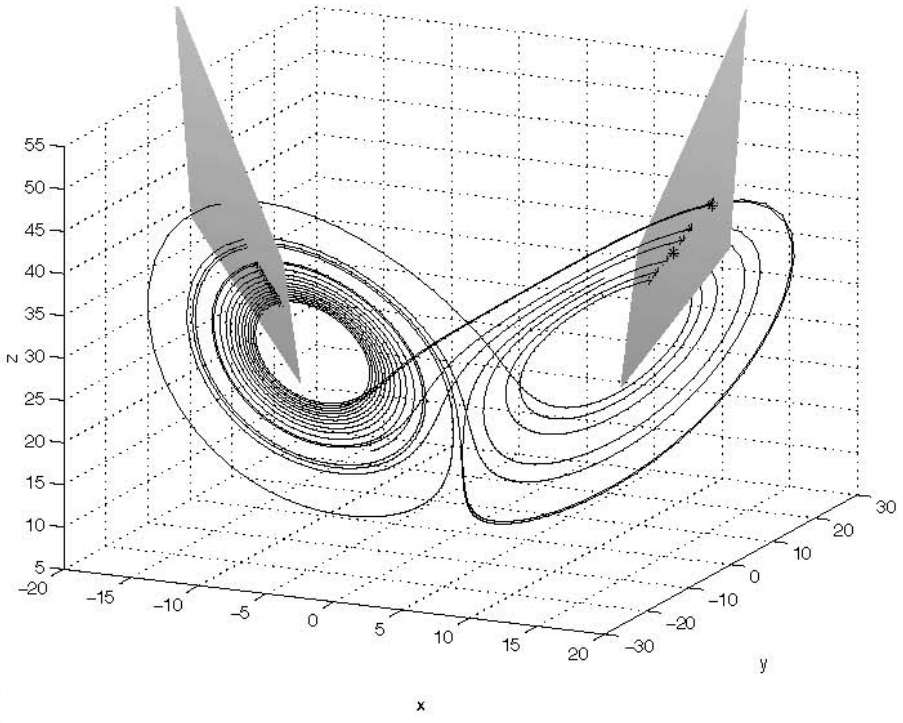

Figure 1.42: Lorenz attractor for $b = \frac{8}{3}$, $\sigma = 10$, and $r = 28$. Maxima of Z are depicted by stars.

Another simple $N = 3$ system which possesses a strange attractor is the Rössler system,

$$\dot{X} = -Y - Z \tag{1.309}$$

$$\dot{Y} = Z + aY \tag{1.310}$$

$$\dot{Z} = b + Z(X - \mu) \ , \tag{1.311}$$

typically studied as a function of μ for $a = b = \frac{1}{5}$. In Fig. 1.44, we present results from work by Crutchfield *et al.* (1980). The transition from simple limit cycle to strange attractor proceeds via a sequence of period-doubling bifurcations, as shown in the figure. A convenient diagnostic for examining this period-doubling route to chaos is the *power spectral density,* or PSD, defined for a function $F(t)$ as

$$\Phi_F(\omega) = \left| \int_{-\infty}^{\infty} \frac{d\omega}{2\pi} \, F(t) \, e^{-i\omega t} \right|^2 = \left| \hat{F}(\omega) \right|^2 \ . \tag{1.312}$$

As one sees in Fig. 1.44, as μ is increased past each critical value, the PSD exhibits a series of frequency halvings (*i.e.* period doublings). All harmonics of the lowest frequency peak are present. In the chaotic region, where $\mu > \mu_\infty \approx 4.20$, the PSD also includes a noisy broadband background.

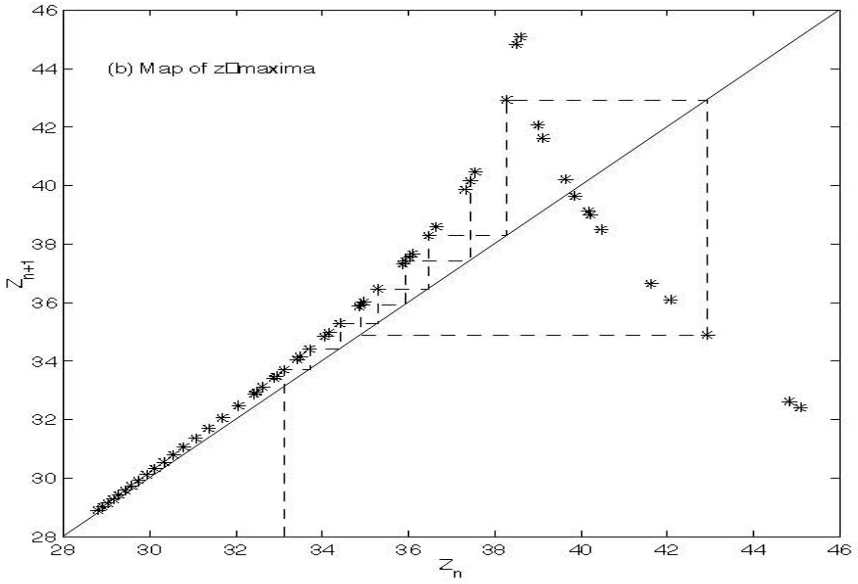

Figure 1.43: Plot of relation between successive maxima Z_n along the strange attractor for the Lorenz system.

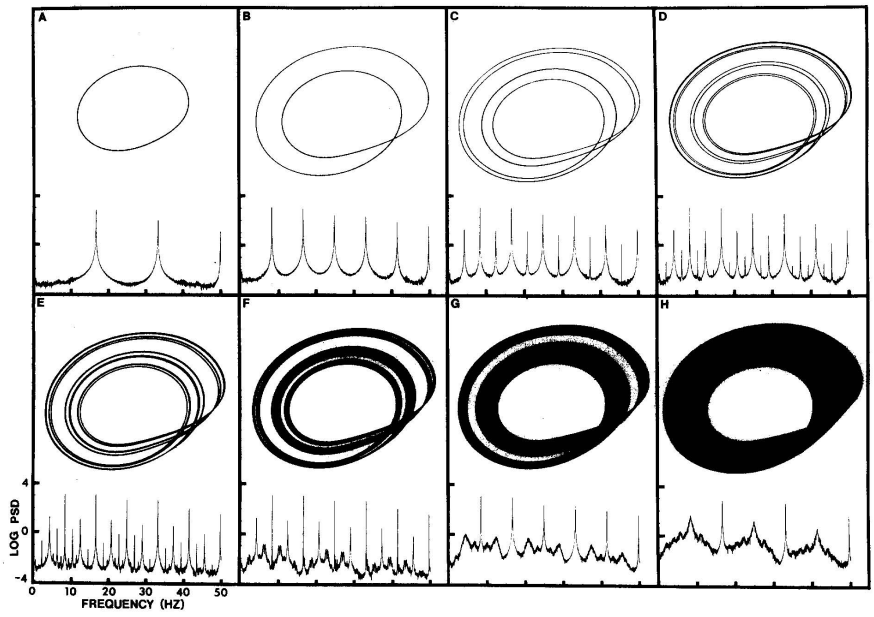

Figure 1.44: Period doubling bifurcations of the Rössler attractor, projected onto the (x, y) plane, for eight values of μ, and corresponding power spectral density for $Z(t)$. (a) $\mu = 2.6$; (b) $\mu = 3.5$; (c) $\mu = 4.1$; (d) $\mu = 4.18$; (e) $\mu = 4.21$; (f) $\mu = 4.23$; (g) $\mu = 4.30$; (h) $\mu = 4.60$.